Train-speed sensitivity approach for maximum response envelopes in dynamics of railway bridges

A. E. Martínez-Castro[a,*], E. García-Macías[b]

[a]E.T.S. Ingenieros de Caminos, Canales y Puertos, Av. Fuentenueva sn 18002. Granada, Spain
[b]Department of Civil and Environmental Engineering, University of Perugia, Via G Duranti 93, Perugia 06125, Italy

Abstract

The design of high-speed railway bridges is strongly conditioned by vibrations and resonance amplifications induced by rail traffic. Furthermore, most current dynamic analysis approaches are computationally expensive, what poses an obstacle to the study of structural alternatives at early design stages. In order to address this limitation, this paper presents a semi-analytic meta-model based on train speed sensitivity analysis. This technique exploits the sensitivity of the dynamic response of bridges to train speed variations or, in other words, the slopes of the maximum response envelopes. The only approximation of this technique stems from the spatial discretization by finite element modelling and modal superposition, while the formulation is closed-form in the time domain. In this way, it is possible to efficiently compute envelope values and sensitivities with moderate train speed sampling frequencies and, afterwards, approximate the remaining speeds through a cubic spline interpolation. Four case studies are presented in order to illustrate the potentials of the proposed technique, including from simply supported beams to complex three-dimensional models. The numerical results report substantial reductions in the computation time and storage requirements, proving the present approach to be a valuable tool for rapidly assessing the performance of design alternatives.

Keywords: Bridge dynamics, Design envelopes, Dynamics of Railway bridges, Meta-model, Semi-analytic solution, Sensitivity analysis, Train-induced vibrations

1. Introduction

High-Speed Lines (HSLs) play a leading role in sustainable mobility policies, due to their lower carbon footprint and higher energy efficiency compared to road and air transport [1]. Nonetheless, the associated infrastructure requires facing complex engineering problems, including the design of railway bridges which constitute especially sensitive assets of the rail network. In particular, the design of high-speed railway bridges is conditioned by train-induced vibrations and resonance amplifications [2]. Such dynamic loads must be considered at the concept design stage when the stiffness/mass distribution and the system damping are defined [3]. However, most current dynamic analysis approaches are computationally demanding, and it is desirable to count on cost-efficient approaches apt for fast evaluations of the performance of design alternatives during train crossings.

The dynamic analysis of railway bridges is a complex endeavour since a broad number of variables and uncertainties are involved [4, 5], including stiffness, mass and damping distributions, bridge supports, train speed, train axle arrangements, existence of track and vehicle irregularities, etc. In general, the dynamic response of railway bridges is often described in terms of Dynamic Amplification Factors (DAFs). Dynamic Amplification Factors represent the dynamic response amplification compared to the static response for a single moving load [6, 7]. A noteworthy research effort was made by the European Research Institute (ERRI) on the dynamics of HSLs in the late 1990s [4]. This was aimed at devising approximate expressions of DAFs, later introduced in Eurocode 1 [6]. Eurocode also proposes a detailed method for determining DAFs, which is applicable for real train loading (Eurocode annex C [6]). A thorough literature review on methodologies for the study of DAFs of highway bridges was provided by Deng and co-authors [8]. With regard to railway bridges, Frỳba [9] proposed simple equations for DAFs considering the resonance condition caused by the train movement on the bridge. The work by Savin [10] derived exact analytical solution for the DAFs of Euler-Bernoulli beams traversed by a succession of massless point loads. Another noteworthy contribution was made by Hamidi and Danshjoo [11] who presented a parametric

*Corresponding author. Department of Structural Mechanics and Hydraulic Engineering. University of Granada. Tel: +34 958 24 95 11; fax: +34 958 24 99 59

Email addresses: amcastro@ugr.es (A. E. Martínez-Castro), \textcolor {black}{enrique.garciamacias@unipg.it} (E. García-Macías)

analysis to investigate the effects of train velocity, train axle distance, number of axles and span lengths on the DAFs of railway steel bridges. That work concluded that the DAFs proposed by current bridge design codes (viz. AREMA [12] and Eurocode [6]) are underestimated and insecure. Goicolea *et al.* [13] investigated the effect of consecutive train passage on resonance phenomenon of railway bridges. Their results demonstrated the Eurocode design manual overestimates the dynamic response of bridges in specific velocities and axle distances.

Current design codes also prescribe limit states regarding maximum accelerations of bridge decks. The awareness on the importance of deck accelerations arose as a consequence of the ballast instability problems observed in the HSL from Paris to Lyon [14]. Subsequent investigations revealed that this phenomenon is associated with vertical accelerations of the deck (of the order of 0.7–0.8 g) produced by the crossing of trains at certain resonant speeds. Along these lines, the Committee D-214 of the ERRI [15, 16] delved into the analysis of the ballast destabilization problem on the basis of shake table testing. Thereby, safety limits for bridge deck accelerations were set and later included in Eurocode 1 [6]. Further research works have been reported in the literature on the dynamic behaviour of ballast within critical frequency ranges (0–30 Hz according to EN1991-2). It is worth noting the laboratory tests conducted by Norris et al [17] and Zacher and Baessler [14] to enhance the criteria provided by Eurocode 1. Moreover, field monitoring of the acceleration response of full-scale railway bridges was performed by Xia and Zhang [18] and Rebelo *et al.* [19].

In the light of the limit states of maximum deck accelerations, the study of the moving-load-induced-vibration problem has focused the attention of researchers during decades. Typically, trains are modelled as tandem systems with massless loads moving with constant velocity. In this case, the equations of motion can be solved using modal superposition or the more time-intensive Newmark's linear integration method (i.e. step-by-step integration). Such approaches are well-suited for bridges with masses considerably exceeding the weight of the train, including concrete bridges as well as steel bridges with ballast or slab tracks [5]. Since the initial closed-form solutions by Bleich [20] for simply supported beams, the formulations have evolved from beam models to general three-dimensional structures. In this respect, the classical references by Frỳba [21, 22] provide a thorough review of the field during the last century. More recent research works can be found in the literature regarding the dynamic response to moving loads of curved beams [23, 24], inclined beams [25], elastic plates [26, 27], composite plates [28, 29], half-space continuum media [30, 31], etc. A comprehensive literature survey was reported by Ouyang [32] concerning the analysis of the moving load problem and related problems. In this context, the semi-analytic solution proposed by Martínez-Castro *et al.* [33] in 2006 represents a noticeable breakthrough in the study of bridges under massless moving loads. While the spatial dimension of the problem is approximated by modal superposition, this approach models the time domain with an analytical closed-form solution. The latter is traced with sampling time steps considerably larger than those required by stable numerical integration schemes. Therefore, the semi-analytic solution primarily outperforms classical step-by-step integration approaches in terms of global computing time.

Notwithstanding the remarkable reported advances, the dynamic analysis of full-scale railway bridges remains an intricate task with vast computational demands. Specifically, the dynamic analysis of railway bridges is aimed at detecting resonant amplifications caused by trains running at design speed ranges. To do so, design envelopes are typically derived by computing the maximum values of certain parameters of interest (e.g. accelerations or displacements) as functions of the train speed. The numerical evaluation of such envelopes is time consuming due to several factors [3]: (i) number of Degrees Of Freedom (DOFs) considered in the structure, (ii) number and complexity of the considered vibration modes (with resonant frequencies up to 30 Hz [6]), (iii) time-step size, (iv) train speed-step size, (v) number of considered trains, and (vi) number of post-processing points. This is particularly critical for low-damped bridges, as it is the case of composite or steel bridges, where time and train speed must be finely sampled to accurately evaluate the dynamics of the structure. To illustrate this, let us ascertain the number of direct calculations that are required to analyse the dynamic behaviour of a low-damped continuous three-span bridge. Generally, the considered train configurations comprise the ten High-Speed Load Models (HSLM-A) of Eurocode 1 [6], as well as other national train compositions (e.g. in the case of the Spanish code IAPF [34], AVE and TALGO trains). Considering a train speed interval ranging from 20 km/h to 420 km/h and a train speed-step $\Delta v = 1$ km/h, 14940 time series ought to be determined followed by the detection of the maximum values at each post-processing point. Given that three ballasted tracks hypotheses must be considered [6], the number of direct evaluations amounts to 44820. All in all, it is evident that the development of cost-efficient dynamic analysis techniques is of pivotal importance for bridge design at initial design stages.

In light of the literature review, this paper is aimed at developing a computationally efficient technique for fast assessment of maximum response envelopes of railway bridges under moving train loads. Typically, dynamic design envelopes are obtained by direct sampling of the maximum response of bridges for a range of train speeds. Nonetheless, this approach is highly time-consuming because of the elevated number of time series required to detect resonant amplifications. Alternatively, this paper proposes a novel meta-model based on Train Speed Sensitivity (TSS) analysis. This methodology exploits the sensitivity of the dynamic response of bridges to train speed variations, that is to say, the slopes of the maximum response envelopes. In this way, it is possible to define a moderate train speed sampling frequency and, afterwards, approximate the non-sampled speeds through a cubic spline interpolation. To do so, the direct problem is first solved by the semi-analytic solution introduced by Martínez-Castro *et al.* [33]. Such formulation is analytical in the time-domain and, therefore, the TSS can be derived in a closed form. In order to illustrate the potentials of the proposed technique, four case studies are presented. These include two different three-span beam models, as well as two three-dimensional bridge structures, namely a composite steel-concrete and a concrete box girder bridge. The numerical results report substantial reductions in the computation times, and the presented approach proves to be a valuable tool for rapidly assessing the performance of structural alternatives at early design stages.

The remaining of this paper is organised as follows. Section 2 overviews the basic semi-analytic solution. Section 3 presents the theoretical formulation of the proposed TSS approach. Section 4 presents the case studies and discussion and, finally, Section 5 concludes this work.

2. The Semi-Analytic solution

This section concisely overviews the semi-analytic solution previously presented in references [33, 35, 36]. Figure 1 sketches the basic configuration of the Finite-Element (FE) mesh of a general three-dimensional bridge. The load lane represents the railway centreline where axle loads are transferred to the structure. A local Cartesian coordinate system $R \equiv \{O; x, y, z\}$ is defined such that the origin O is located at the initial point of the load lane, x-axis is the longitudinal direction, y-axis is a transverse axis, and z-axis represents the vertical direction perpendicular to the bridge deck. A single point moving load P traverses the bridge at a constant speed v. The resulting time-dependent load can be formally written as $p(x,t) = P\delta(x - vt)$, with δ being the Dirac delta function and t time. Note that, assuming linearity, the solution for a train of loads can be simply obtained by adding the contributions of every single load. On this basis, let us focus the formulation to the one single load case.

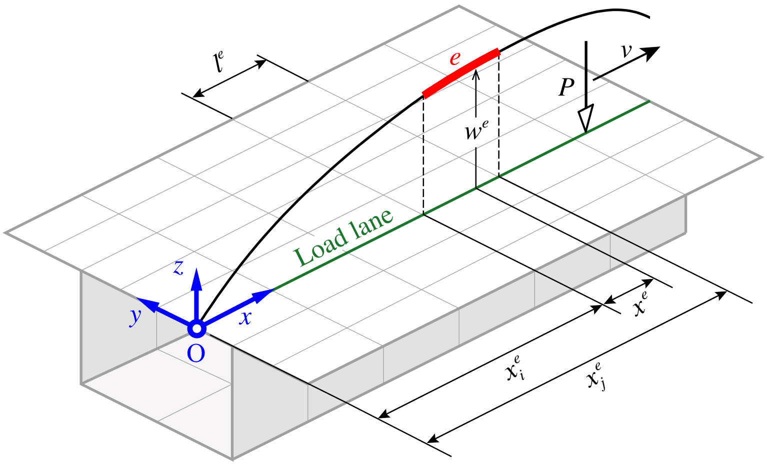

Figure 1: General bridge structure under one single moving load, and cubic spline interpolation of displacements along the load lane.

Let be the finite element $e \equiv \left\{x : x \in \left[x_i^e, x_j^e\right]\right\}$ lying along the load lane, with x_i^e and x_j^e denoting the spatial x-coordinates of its initial and final nodes, respectively. Also, let x^e be the abscissa relative to the origin of the element, i.e. $x^e = x - x_i^e$. For clarity purposes, the solution is given for a unitary load ($P = 1$) although, assuming a linear behaviour of the system, the solution for a different load can be simply computed by multiplying the former one by the actual value of P. On this basis, the vertical displacement $w^e(x, y, z, t)$ of an arbitrary point (x, y, z) on the element e can be obtained by modal expansion as:

$$w^e(x, y, z, t) = \sum_{n=1}^{m} q_n(t)\, \phi_n^e(x, y, z), \tag{1}$$

where the term $q_n(t)$ denotes the n-th time-dependent modal amplitude or generalized coordinate, and $\phi_n^e(x, y, z)$ is the n-th mode shape evaluated at (x, y, z). The number of considered modes, m, is usually prescribed by design codes. In particular, Eurocode 1 [6] sets this limit as the number of modes with resonant frequencies below 30 Hz.

It is considered that the FE mesh enables the consideration of equivalent 1D beam-type DOFs along the load lane. Strictly speaking, it is assumed that the displacement field of an arbitrary point in a segment of the lane is determined by the displacements, w, and slopes, $\theta_x = \partial w/\partial x$, at the discretized nodes. On this basis, the displacement pattern along the load lane can be characterised by a Hermite cubic spline. Therefore, a spatial discretization along the load lane can be defined by using the Hermite shape functions, $h_i(x^e)$, in such a way that Eq. (1) is rewritten with no explicit dependence on variables y and z as:

$$w^e(x^e, t) = \sum_{n=1}^{m} q_n(t) \sum_{i=1}^{4} G^e_{ni}\, h_i(x^e), \tag{2}$$

where the matrix coefficients G^e_{ni} are functions of the modal coordinates, and represent the evaluation of the mode shapes along the load lane. In addition, as demonstrated in reference [33], the functions $q_n(t)$ can be obtained in a closed form as the combination of an homogeneous and particular solutions, $q_n(t) = q^h_n(t) + q^p_n(t)$, given by:

$$q^h_n(\tau) = \mathrm{e}^{-\zeta_n\omega_n\tau}\left[A_n\cos\left(\omega^d_n\tau\right) + B_n\sin\left(\omega^d_n\tau\right)\right], \tag{3}$$

$$q^p_n(\tau) = \alpha^{(0)}_n + \alpha^{(1)}_n(v\tau) + \alpha^{(2)}_n(v\tau)^2 + \alpha^{(3)}_n(v\tau)^3, \tag{4}$$

with $\tau = t - x^e_i/v$ being the local time at segment e, and A_n and B_n coefficients of the homogeneous solution. The term $\omega^d_n = \omega_n\sqrt{1-\zeta^2_n}$ in Eq. (3) stands for the damped natural angular frequency of the *n-th* mode, with ζ_n being its damping rate. The coefficients $\alpha^{(i)}_n$ in Eq. (4) are defined as:

$$\begin{aligned}
\alpha^{(0)}_n &= v^3\alpha^{(01)}_n + v^2\alpha^{(02)}_n + v\alpha^{(03)}_n + \alpha^{(04)}_n,\\
\alpha^{(1)}_n &= v^2\alpha^{(11)}_n + v\alpha^{(12)}_n + \alpha^{(13)}_n,\\
\alpha^{(2)}_n &= v\alpha^{(21)}_n + \alpha^{(22)}_n,\\
\alpha^{(3)}_n &= \alpha^{(31)}_n,
\end{aligned} \tag{5}$$

where the ten coefficients $\alpha^{(ij)}_n$ are given in reference [33]. It is important to indicate that these coefficients only depend on the modal properties (i.e. mode shapes, natural frequencies and damping ratios) and the length of the load lane segment. Moreover, the coefficients A_n and B_n in Eq. (3) are obtained from the initial conditions $q^0_n = q_n(0)$ and $\dot{q}^0_n = \dot{q}_n(0)$, with overdots denoting time derivatives, as follows:

$$A_n = q^0_n - \alpha^0_n, \tag{6}$$

$$B_n = \frac{\dot{q}^0_n + \zeta_n w_n A_n - \alpha^{(1)}_n v}{w^d_n}. \tag{7}$$

The complete closed-form solution is constructed in a piecewise form, with an analytical function for each element. At-rest conditions are commonly imposed for the initial time $t = 0$, that is to say, $q^0_n = 0$ and $\dot{q}^0_n = 0$. For the following elements, the initial conditions for element $e+1$ are given by the end values of element e, i.e. $q_n(\tau)|^{e+1}_{\tau=0} = q_n(\tau)|^{e}_{\tau=l^e/v}$ and $\dot{q}_n(\tau)|^{e+1}_{\tau=0} = \dot{q}_n(\tau)|^{e}_{\tau=l^e/v}$.

Finally, the approximate velocity and acceleration are obtained by differentiation of $w^e(x,t)$ in Eq. (1) with respect to time as:

$$\dot{w}^e(x, y, z, t) = \sum_{n=1}^{m} \dot{q}_n(t)\phi^e_n(x, y, z), \tag{8}$$

$$\ddot{w}^e(x, y, z, t) = \sum_{n=1}^{m} \ddot{q}_n(t)\phi^e_n(x, y, z). \tag{9}$$

3. Train Speed-Sensitivity (TSS) approach

In this section, a novel TSS approach for maximum response envelopes is introduced on the basis of the semi-analytic solution overviewed above. Figure 2 illustrates the main concept of the proposed technique. With reference to any dynamic magnitude, such as the vertical acceleration at a fixed point, classical design envelopes are constructed by direct sampling at a discrete set of train speeds. This approach is highly time-consuming due to the elevated number of time series evaluations that are required.

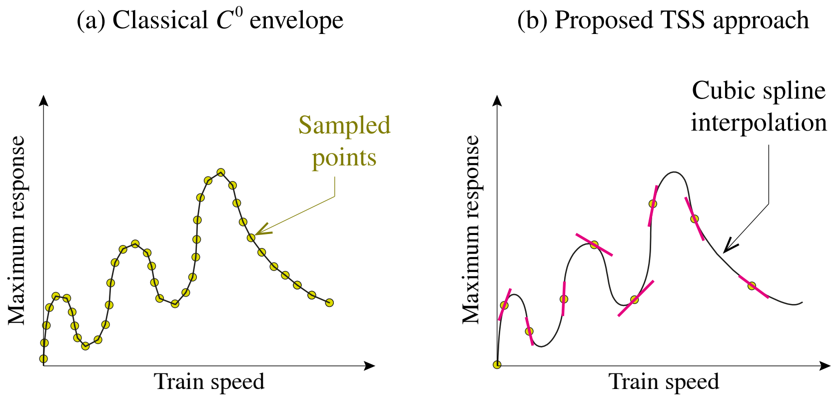

Figure 2: Classical C^0 approximation (a) and proposed TSS approach for maximum response envelopes (b).

As a meta-model, the present TSS approach proposes a C^1 cubic spline interpolation of the design envelopes. To do so, it is necessary to compute the slope of the envelope curve (i.e. its train speed sensitivity) at every sampled train speed. In this way, the number of sampling points can be smaller than those required in the classical C^0 approach and, as a result, substantial reductions in computational burden can be achieved. Furthermore, in virtue of the analytical definition of the semi-analytic approach in the time domain, the train speed sensitivities can be also derived in an analytical closed form.

The remaining of this section introduces the mathematical formulation of the proposed approach. Firstly, Subsection 3.1 furnishes the details on the determination of the TSS of the dynamic response of bridges under one single moving load. Afterwards, Subsection 3.2 extends the previous solution to multiple load trains. Finally, Subsection 3.3 defines the TSS of the maximum response envelope curves, that is to say, the slope of the design envelope curves.

3.1. Train speed sensitivity for one single moving load

The semi-analytical solution introduced in Eqs. (1) to (5) shows an explicit dependence on the train speed, v. Hence, the sensitivity of the displacements field in Eq. (2) with respect to the train speed can be obtained by direct differentiation as:

$$\frac{\partial w^e(x^e, v, t)}{\partial v} = \sum_{n=1}^{m} \frac{\partial q_n(v,t)}{\partial v} \sum_{i=1}^{4} G^e_{ni}\, h_i(x^e). \tag{10}$$

Note that the generalized coordinate function $q_n(v, t)$ depends upon the relative time $\tau = t - x^e_i/v$ (see Eqs. (3) and (4)). Thus, its partial derivative can be written as (if $v \neq 0$):

$$\frac{\partial q_n(v,t)}{\partial v} = \frac{\partial q_n(v,\tau)}{\partial v} + \frac{\partial \tau}{\partial v}\frac{\partial q_n(v,\tau)}{\partial \tau} = \frac{\partial q_n(v,\tau)}{\partial v} + \frac{x^e_i}{v^2}\frac{\partial q_n(v,t)}{\partial t}. \tag{11}$$

It is noted that the second term on the right-hand side of Eq. (11) is directly given by the semi-analytic solution ($\dot{q}_n(t)$). On the other hand, considering the decomposition of the solution $q_n(t) = q^h_n(t) + q^p_n(t)$, the first term on the right-hand side can be expanded as follows:

$$\frac{\partial q_n(v,\tau)}{\partial v} = \frac{\partial q^h_n(v,\tau)}{\partial v} + \frac{\partial q^p_n(v,\tau)}{\partial v}. \tag{12}$$

In virtue of the explicit dependence of Eqs. (3) and (4), the partial derivatives in Eq. (12) can be readily obtained. Firstly, the train speed sensitivity of the homogeneous solution can be expressed after some manipulation as:

$$\frac{\partial q^h_n(v,\tau)}{\partial v} = \mathrm{e}^{-\zeta_n w_n \tau}\left[D_n \cos\left(w^d_n \tau\right) + E_n \sin\left(w^d_n \tau\right)\right]. \tag{13}$$

In a similar way, the train speed sensitivity of the particular solution can be written in a compact way as:

$$\frac{\partial q^p_n(v,\tau)}{\partial v} = \beta^{(0)}_n + \beta^{(1)}_n (v\tau) + \beta^{(2)}_n (v\tau)^2 + \beta^{(3)}_n (v\tau)^3, \tag{14}$$

$$
\begin{aligned}
\beta_n^{(0)} &= 3v^2\alpha_n^{(01)} + 2v\alpha_n^{(02)} + \alpha_n^{(03)},\\
\beta_n^{(1)} &= 3v\alpha_n^{(11)} + 2\alpha_n^{(12)} + \alpha_n^{(13)}/v,\\
\beta_n^{(2)} &= 3\alpha_n^{(21)} + 2\alpha_n^{(22)}/v,\\
\beta_n^{(3)} &= 3\alpha_n^{(31)}/v.
\end{aligned}
\tag{15}
$$

Parameters D_n and E_n in Eq. (13) denote the train speed sensitivity of terms A_n and B_n, respectively. By differentiation of Eqs. (6) and (7) along with the definitions in Eq. (15), one can write:

$$
D_n = \frac{\partial A_n}{\partial v} = \frac{\partial q_n^0}{\partial v} - \beta_n^0 - \frac{x_i^e}{v^2} q_n^0, \tag{16}
$$

$$
E_n = \frac{\partial B_n}{\partial v} = \frac{\frac{\partial \dot{q}_n^0}{\partial v} + \zeta_n w_n D_n - \beta_n^{(1)} v - \frac{x_i^e}{v^2}\dot{q}_n^0}{w_n^d}. \tag{17}
$$

It is interesting to note that Eqs. (13) and (14) have the same structure as Eqs. (3) and (4), respectively. Likewise, coefficients $\beta_n^{(i)}$ in Eq. (15) also exhibit a similar configuration to $\alpha_n^{(i)}$ in Eq. (5). Therefore, the way the TSS of the homogeneous and particular terms is computed and stored is completely analogous to that of the forward solution. Also, the complete TSS is also constructed in a piecewise form with a closed-form analytical function for each element. In this case, at-rest conditions are defined as $q_n^0 = 0$, $\dot{q}_n^0 = 0$, $\partial q_n^0/\partial v$=0 and $\partial \dot{q}_n^0/\partial v$=0. For the following elements, new inter-element compatibility conditions must be included as follows:

$$
\begin{aligned}
\partial q_n/\partial v(\tau)|_{\tau=0}^{e+1} &= \partial q_n/\partial v(\tau)|_{\tau=l^e/v}^{e},\\
\partial \dot{q}_n/\partial v(\tau)|_{\tau=0}^{e+1} &= \partial \dot{q}_n/\partial v(\tau)|_{\tau=l^e/v}^{e}.
\end{aligned}
$$

Finally, the TSS of the velocity and acceleration are obtained by time differentiation of $\partial w^e(x^e, v, t)/\partial v$ in Eq. (10) as:

$$
\frac{\partial \dot{w}^e(x^e, v, t)}{\partial v} = \sum_{n=1}^{m} \frac{\partial \dot{q}_n(v,t)}{\partial v} \sum_{i=1}^{4} G_{ni}^e\, h_i(x^e), \tag{18}
$$

$$
\frac{\partial \ddot{w}^e(x^e, v, t)}{\partial v} = \sum_{n=1}^{m} \frac{\partial \ddot{q}_n(v,t)}{\partial v} \sum_{i=1}^{4} G_{ni}^e\, h_i(x^e). \tag{19}
$$

3.2. Train speed sensitivity for a set of moving loads

The solution for a complete train comprising n_l moving axle loads can be obtained by superposition. To do so, the number of loads that have already crossed the lane, n_o, those upon the bridge, n_i, and those that have not yet entered the structure, n_s, must be monitored at each time step ($n_l = n_s + n_i + n_o$). Each moving load k is characterized by a load value, P_k, and a distance from the origin of the structure, d_k. Hence, Eq. (11) must be accordingly expanded into two terms as follows:

$$
\frac{\partial q^n}{\partial v}(t) = \left.\frac{\partial q^n}{\partial v}\right|_{in}(t) + \left.\frac{\partial q^n}{\partial v}\right|_{out}(t), \tag{20}
$$

where subscripts "*in*" and "*out*" relate the corresponding quantity to the axle loads upon the bridge and those that have already left the structure, respectively. Let superscript "*e*" denote the element of the lane discretization ($e \in [1, N]$) in which a k-th axle load is located at a distance xi^e from its origin at time t. Therefore, the relative time for the k-th load can be defined as $\tau_k = t - \left(d_k + x_i^e\right)/v$. If the k-th load has abandoned the structure, the relative time takes the expression $\tau_k^{N+1} = t - \left(d_k + x_j^N\right)/v$. In this light, the contributions of the axle loads upon the structure and those that have already abandoned it can be written as:

$$
\begin{aligned}
\left.\frac{\partial q^n}{\partial v}\right|_{in}(t) = \sum_{k=n_o+1}^{n_o+n_i} \Big\{ & \mathrm{e}^{-\zeta_n w_n \tau_k} \left[D_n \cos\left(w_n^d \tau_k\right) + E_n \sin\left(w_n^d \tau_k\right)\right] + \beta_n^{(0)} + \beta_n^{(1)}(v\tau_k) + \\
& + \beta_n^{(2)}(v\tau_k)^2 + \beta_n^{(3)}(v\tau_k)^3 + \frac{d_k + x_i^e}{v^2}\dot{q}_k(t) \Big\} P_k,
\end{aligned}
\tag{21}
$$

$$\left.\frac{\partial q^n}{\partial v}\right|_{out}(t) = \sum_{k=1}^{n_o}\left\{\mathrm{e}^{-\zeta_n w_n \tau_k^{N+1}}\left[D_{N+1}\cos\left(w_n^d\tau_k^{N+1}\right) + E_{N+1}\sin\left(w_n^d\tau_k^{N+1}\right)\right] + \frac{d_k + x_j^N}{v^2}\dot{q}_k(t)\right\}P_k, \tag{22}$$

where coefficients D_{N+1} and E_{N+1} are selected so that the compatibility of the solution is enforced in free vibration once the loads have crossed the bridge.

All in all, the solution procedure can be summarised as follows:

(i) Resolution of the generalized eigenvalues problem of the FE numerical model to determine the mode shapes, ϕ_n^e, and resonant frequencies, ω_n. Thereby, the matrix coefficients G_{ni}^e in Eq. (2) are obtained as the evaluation of the mode shapes along the load lane.

(ii) Coefficients $\alpha_n^{(ij)}$ are computed and stored for the entire mesh and all the modes considered in the analysis.

(iii) For a given train speed, the coefficients of the homogeneous solutions $[A_n, B_n, D_n, E_n]_{e=1}^{N+1}$, and of the particular solutions $\left[\alpha_n^0, \alpha_n^1, \alpha_n^2, \alpha_n^3\right]_{e=1}^{N+1}$ and $\left[\beta_n^0, \beta_n^1, \beta_n^2, \beta_n^3\right]_{e=1}^{N+1}$ are calculated and stored for each mode and element.

(iv) At every time step t, the number of axle loads n_o and n_i are computed. Afterwards, the solutions given by Eqs. (20) to (22) are computed for each mode and, finally, the overall solution is obtained by modal superposition as indicated in Eq. (2).

3.3. Train speed sensitivity of maximum response envelopes

In practice, envelope design curves require sampling speed intervals fine enough to capture resonant amplification phenomena, what typically results in considerable computational costs. The present approach replaces the classical forward C^0 interpolation by a cubic interpolation approximation as previously sketched in Fig. 2. This permits larger train speed steps, avoiding time series to be sampled at intermediate speeds and, as a result, yielding substantial computational cost reductions.

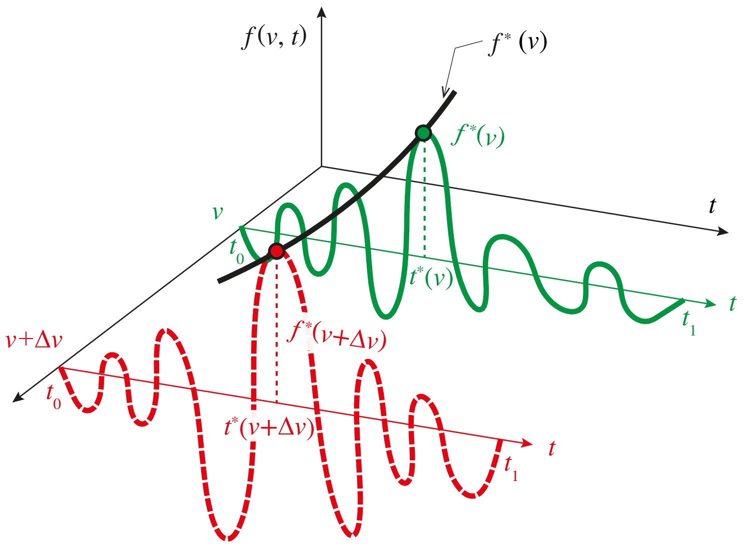

Figure 3: Local evolution of the global maximum of the dynamic response.

Once the time series of the train speed sensitivity of the dynamic magnitude of interest are computed, it is necessary to determine the slope of the maximum response design envelope. To do so, it is required to perform a local analysis as illustrated in Fig. 3. Let $f(v,t)$ be a function of interest dependent on the train speed $v \in [V_0, V_1]$ and time $t \in [t_0, t_1]$. Typically, the function $f(v,t)$ represents oscillating displacement and acceleration time series. The primary goal of the dynamic analysis of railway bridges under train actions is the determination of the maximum response envelope, $f^*(v)$, which can be formally written as:

$$f^*(v) = \sup_{t\in[t_0,t_1]} f(v,t) = f(v, t^*(v)), \tag{23}$$

where $t^*(v)$ denotes the time values where the local maximum of $f(v,t)$ takes place at every train speed. The local evolution of $f^*(v)$ in a small neighbourhood of train speeds $(v, v+\Delta v)$ is represented in Fig. 3. The aim of this work is to determine the train speed sensitivity of the maximum response function, that is $\partial f^*(v)/\partial v$. In virtue of the *envelope theorem* (see e.g. [37–39]), it can be proven that such partial derivative reads:

$$\frac{\partial f^*(v)}{\partial v} = \lim_{\Delta v \to 0} \frac{f(v+\Delta v, t^*(v+\Delta v)) - f(v, t^*(v))}{\Delta v} = \lim_{\Delta v \to 0} \frac{f(v+\Delta v, t^*(v)) - f(v, t^*(v))}{\Delta v}, \tag{24}$$

or, in other words, the local extreme value $f^*(v+\Delta v)$ occurs at time $t^*(v)$.

In this light, the procedure of the proposed TSS approach for maximum response envelopes can be summarised as follows. At every sampled train speed, the maxima of the dynamic magnitudes (displacements or accelerations) are searched by sampling the time series on the basis of the semi-analytic solution presented in Section 2. Additionally, time instants $t^*(v)$ where local maxima take place are collected so that the pair $(f^*(v), t^*(v))$ is stored for every time series. On the basis of the result above, the slopes of the envelope design curves are computed by evaluating the solution presented in Subsection 3.2 at instant times $t^*(v)$. In this way, the pair $(f^*, \partial f^*/\partial v)$ is computed and stored at every sampled train speed. Finally, the envelope values of non-sampled intermediate train speeds are extracted by a cubic spline between every two consecutive sampled points. In this work, the proposed technique has been implemented in a FORTRAN computer code and all the numerical simulations presented hereafter have been obtained on a standard desktop PC equipped with an AMD Athlon XP 2000 processor and a DDR 266 MHz RAM memory.

4. Case studies and discussion

In this section, the effectiveness of the proposed Train-Speed Sensitivity (TSS) meta-model is assessed in four different case studies. Firstly, a three-span continuous stepped beam is used as a validation case in Section 4.1. In this case, the present approach is benchmarked against results from direct-time integration using the implicit Newmark-beta method. Subsequently, the one-dimensional three-span bridge reported in Eurocode 1 is used as a case study in Section 4.2. Finally, Sections 4.4 and 4.3 further investigate the application of the proposed approach to three-dimensional bridge structures, including a composite steel-concrete bridge and a concrete box girder bridge, respectively.

4.1. Validation case: three-span continuous stepped beam.

In this first set of analyses, a three-span continuous stepped beam retrieved from the literature [33, 40] is used as validation case. The structure is sketched in Fig. 4 and consists of a 20 m length three-span continuous stepped beam with a constant mass per unit length ρA of 1000 kg/m, and a constant modal damping ratio ζ of 2%. The flexural stiffness EI is 1.96 GNm^2 in the lateral spans, while it is doubled in the central one. In addition, two different moving load cases are considered as shown in Fig. 5. The first load case is labelled LC-1 and consists of a single point load of 9.8 kN crossing the beam at a constant speed v. On the other hand, the load case LC-2 consists of two point moving loads of 9.8 kN, located 5 m and 15 m far from the origin of the beam at t=0, respectively. For validation purposes, the beam is also modelled with the commercial FE code SAP2000 and its dynamic response is computed by the implicit direct-time integration method of Newmark-beta with modal superposition. In the simulations, the first twelve modes of vibration are considered. In addition, the time step size Δt is selected as $T_{12}/10$, with T_{12} being the period of the twelfth mode of value 0.77 ms.

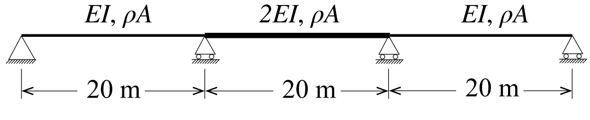

Figure 4: Geometry and stiffness properties of the three-span continuous stepped beam (ρA=1000 kg/m, EI=1.96 GNm^2, ζ=2%).

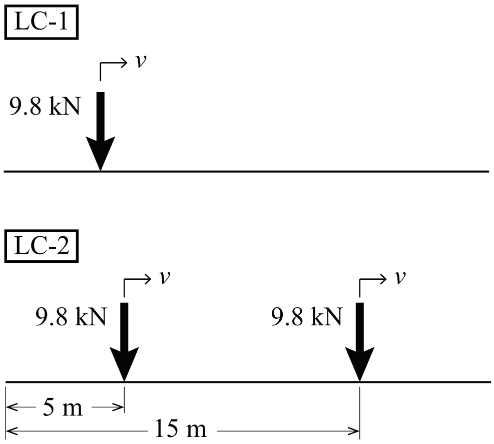

Figure 5: Moving load cases considered in the validation case of a three-span continuous stepped beam.

251 Figs. 6 and 7 depict the load speed sensitivity of the vertical acceleration in the the mid-span point of the first span for load cases LC-1 and LC-2, respectively, and considering a load speed of v=130 km/h. In addition, the load speed sensitivity is also computed by the Newmark-beta method to serve as a validation basis. To this end, the load speed sensitivity ($\partial a/\partial v$) is computed through central finite differences of the Newmark-beta's solutions at speed intervals of Δv=0.1 km/h, labelled as NFD in the figures. Excellent agreements can be observed in both cases and, therefore, these results demonstrate the correctness of the present approach.

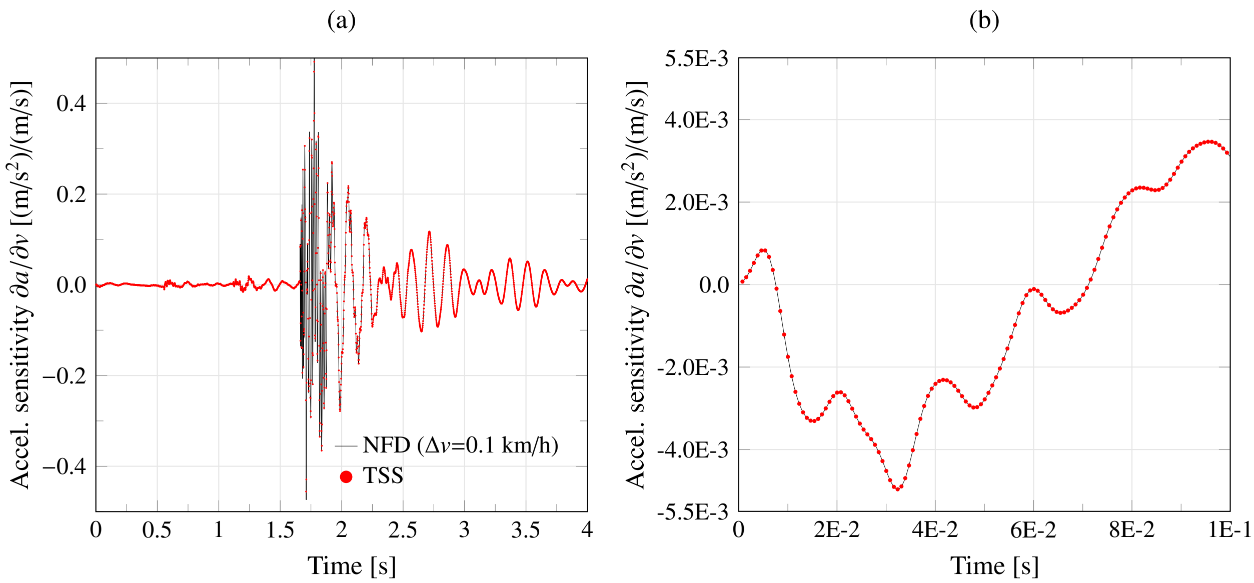

Figure 6: General (a) and detailed view (b) of the time series of train speed sensitivity of the vertical acceleration of the mid-span point of the first span of the three-span continuous stepped beam under LC-1. NFD stands for the the finite differences of the Newmark-beta's solution used for validation purposes (v=130 km/h, Δt=7.7E-4 s).

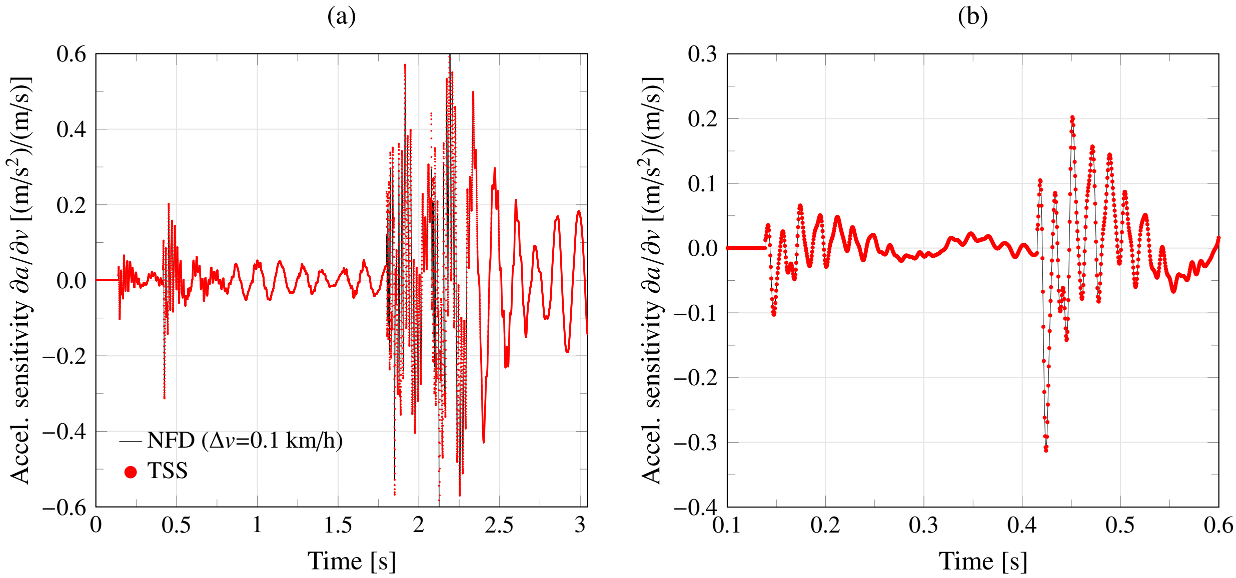

Figure 7: General (a) and detailed view (b) of the time series of train speed sensitivity of the vertical acceleration of the mid-span point of the first span of the three-span continuous stepped beam under LC-2. NFD stands for the the finite differences of the Newmark-beta's solution used for validation purposes (v=130 km/h, Δt=7.7E-4 s).

Finally, the correctness of the proposed TSS approach in combination with the cubic interpolation of the maximum/minimum response envelopes is investigated in Figs. 8 and 9. To do so, the results of the present approach in terms of maximum/minimum accelerations are benchmarked against the forward sampling of the semi-analytical solution (FS). The present approach is evaluated for varying load speed steps, namely Δv=5 km/h, 10 km/h, 15 km/h and 20 km/h. On the other hand, the semi-analytic solution is computed considering small load speed increments of Δv=1 km/h in order to finely trace the envelopes. On this basis, Figs. 8 and 9 furnish the envelope curves of maximum/minimum accelerations in the mid-span point of the first span of the three-span continuous stepped beam under the load cases LC-1 and LC-2, respectively. In general, it is noted that the present approach yields estimates that are decreasing in accuracy for higher load speed steps. The origin of such discrepancies primarily depends upon the smoothness of the envelope curves or, alternatively, the degree of approximation of the cubic spline interpolation to the actual envelope. Fig. 8 (a) is an illustrative example of this. It is observed that the curves computed by the TSS meta-model are tangent to the envelope curve at the sampled velocities, a fact that evidences that the present approach accurately captures the load speed sensitivity of the envelope. Nonetheless, noticeable discrepancies arise in some local maxima such as the one located around 170 km/h. Here, the TSS curves for Δv=5 km/h and 10 km/h yield maximum accelerations very close to the semi-analytic solution unlike those for Δv=15 km/h and 20 km/h. In the latter cases, considerably larger differences can be observed as a result of insufficient sampling rates. All in all, it is concluded that the TSS meta-model with moderate sampling rates (Δv=5 km/h and 10 km/h in this case) effectively provides a fast evaluation of the maximum/minimum response envelopes of bridge structures under moving train loads.

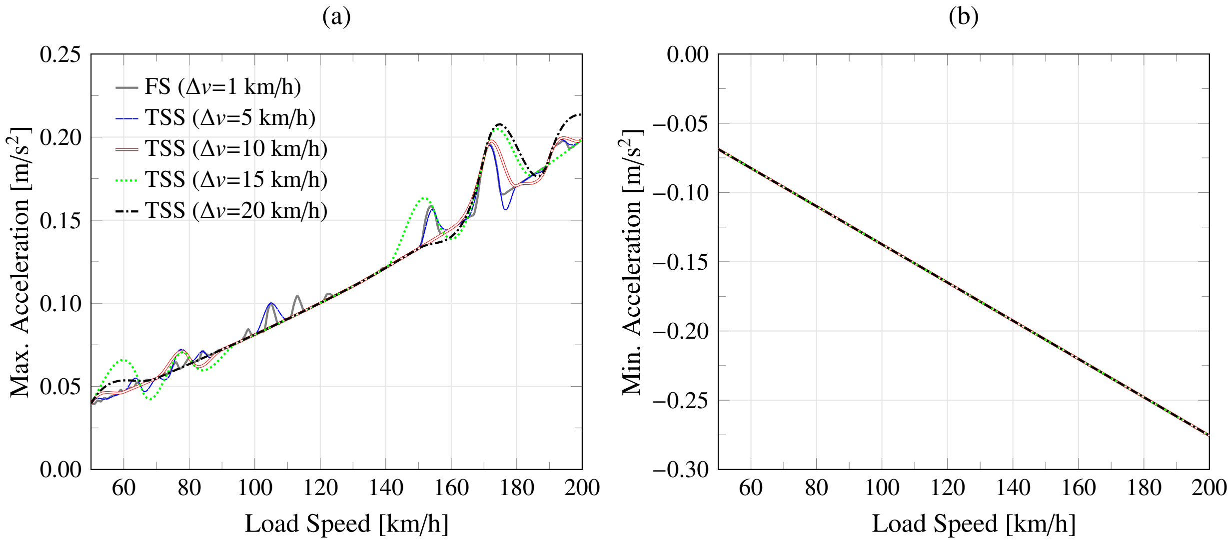

Figure 8: Envelopes of maximum (a) and minimum (b) accelerations in the mid-span point of the first span of the three-span continuous stepped beam under LC-1 (Δt=7.7E-4 s).

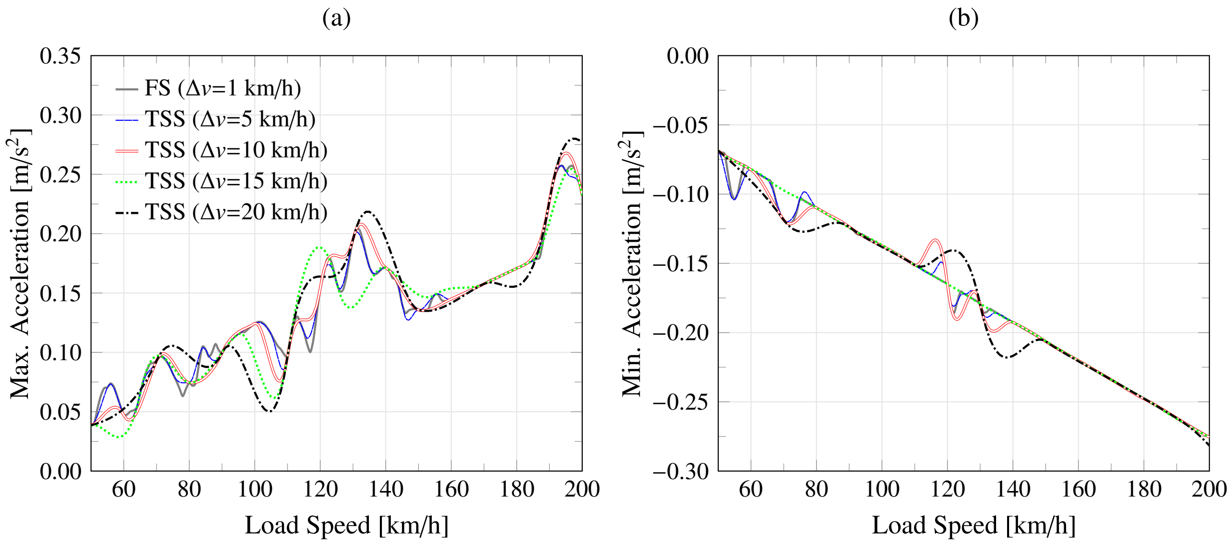

Figure 9: Envelopes of maximum (a) and minimum (b) accelerations in the mid-span point of the first span of the three-span continuous stepped beam under LC-2 (Δt=7.7E-4 s).

4.2. *Case study I: continuous three-span bridge from Eurocode 1.*

This first case study is aimed at illustrating the effectiveness of the proposed TSS meta-model to provide fast evaluations of maximum response envelopes of bridges under complex moving train loads. In particular, a continuous three-span high-speed bridge analysed in Eurocode 1 [6] is selected as a case study. The bridge is sketched in Fig. 10 and consists of two 25 m long lateral spans and a 30 m long central one. The bridge is modelled in SAP2000 with ten Euler-Bernoulli beam elements per span with constant mass per unit length ρA=14435.25 kg/m, and flexural stiffness EI=110649.6 MNm^2. A modal analysis of the bridge is conducted and the first five modes with resonant frequencies below 30 Hz are retained for the subsequent simulations. The bridge is also assumed to be low-damped with a modal damping ratio of ζ=1%.

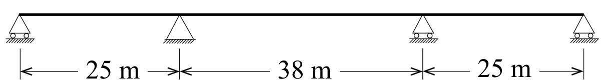

Figure 10: Continuous three-span bridge proposed in Eurocode 1 [6].

Figure 11 shows the minimum/maximum acceleration envelopes of the mid-span of the central span under the passage of the ten trains of the HSML-A model of Eurocode 1 at speeds ranging from 144 to 422 km/h. The estimates of the TSS meta-model are computed considering train speed steps of 10 km/h and time steps of $T_5/10$=6.3E-3 s, with T_5 being the period of the fifth mode of vibration. Let us recall that the proposed TSS meta-model is analytical in the time domain, whereby the criteria for determining the time sampling merely attend to resolution needs, while errors stemming from time integration are nonexistent. For comparison purposes, the results provided by the semi-analytic approach are also shown with train speed steps of 1 km/h. In both cases, the minimum/maximum accelerations are extracted from the response time series, including the train passage time and a free vibration time of six times the highest period of the structure. In Fig. 11, excellent agreements are found between the two used methods. Although slight discrepancies can be observed around local minima/maxima such as those around 310 km/h, the proposed TSS meta-model is shown to accurately capture the global minima/maxima around 277 km/h. The latter corresponds to the resonant train speed dominated by the fundamental bending mode with natural frequency of 4.28 Hz. In general, given that only a limited number of vibration modes usually determine the dynamic response of bridges at resonant speeds, the speed sensitivity is specially well captured in the vicinity of resonances. Hence, it can be concluded that the proposed TSS approach is well-suited for detecting resonant peaks.

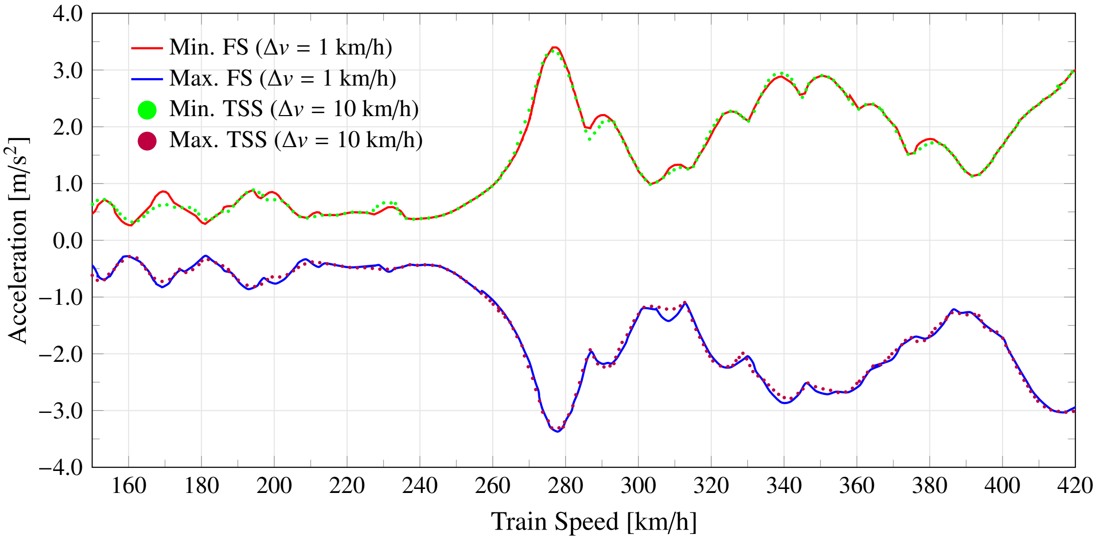

Figure 11: Maximum/minimum acceleration envelopes at mid-span of the central span of the continuous three-span bridge from Eurocode 1 under the passage of the ten trains of the HSML-A model of Eurocode 1.

In virtue of the analytic closed-form definition of train speed sensitivity in the present approach, the observed discrepancies with the semi-analytic estimates are simply ascribed to insufficient sampling of the response envelopes. In order to illustrate this, Fig. 12 depicts the absolute envelope values of acceleration computed by the TSS meta-model with varying train speed steps, namely Δv=10 km/h and 20 km/h. It is observed in this figure that the train speed sensitivity is accurately captured in all the cases, that is to say, the estimated envelopes are tangent to the actual envelope at every sampling point. Hence, the observed discrepancies for increasing train speed steps are simply due to insufficient sampling issues. It is also important to note that the sampling errors are considerable lower at global maxima.

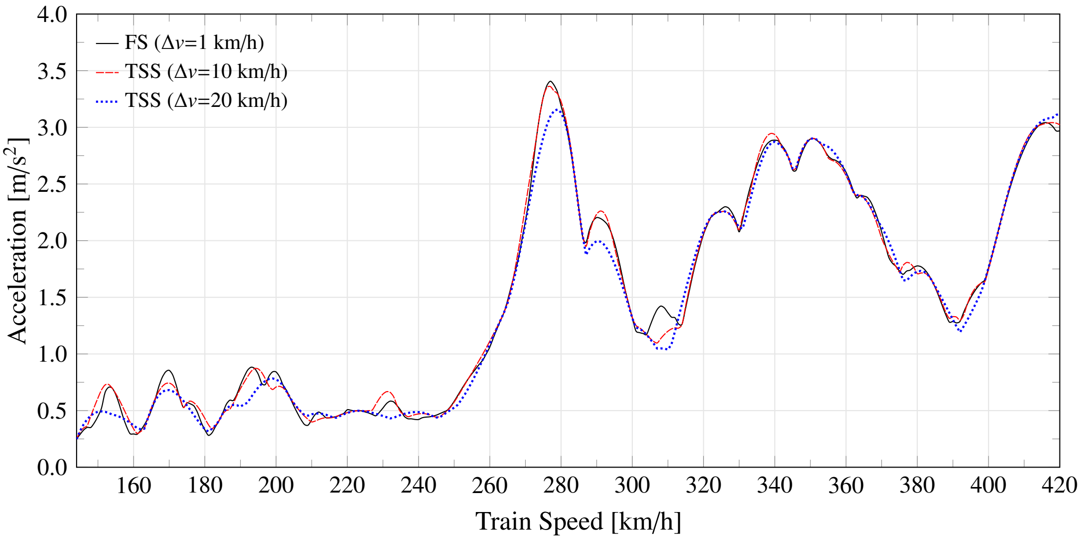

Figure 12: Maximum absolute acceleration envelopes at mid-span of the central span of the continuous three-span bridge from Eurocode 1 under the passage of the ten trains of the HSML-A model of Eurocode 1.

Finally, the robustness of the proposed meta-model for increasing train speed steps Δv is investigated in Fig. 13. In order to further extend the analysis, in addition to the previously defined damping ratio $\zeta = 1.0\%$, two more damping ratios are also considered, namely $\zeta = 0.5\%$ and $\zeta = 2.0\%$ representing the commonly used values in the design of steel-concrete composite and concrete bridges, respectively. As reference solutions, the maximum acceleration envelopes at mid-span of the central span under the passage of the ten trains of the HSML-A model are obtained through forward sampling with $\Delta v = 1$ km/h as shown in Fig. 13 (a). Note that the maximum acceleration at the resonant speed (≈ 275 km/h) increases considerably for decreasing damping ratios (2.2 to 4.6 m/s^2 for damping ratios $\zeta = 0.5\%$ and $\zeta = 2.0\%$, respectively). Furthermore, given that the contribution of high-frequency vibration modes is larger for low-damped bridges, the design envelopes are less smooth in these cases. The relative errors (RE) of the estimates of the maximum acceleration by FS and the proposed TSS meta-model are depicted in Fig. 13 (b) for the afore-mentioned damping ratios. In all cases, it is observed that the proposed meta-model is more stable that the forward sampling of the acceleration envelopes. A closer inspection reveals that the proposed meta-model yields slight overestimates of the actual values for low speed steps due to the cubic interpolation, while the FS approach always leads to underestimates derived from sampling errors. In order to quantitatively assess the robustness of both approaches, a comparison magnitude is defined as the minimum speed step that is necessary to obtain estimates above 95% of the actual value. In the case of the FS approach, minimum speed steps of 8 km/h are obtained for all the considered damping ratios. Conversely, in the case of the proposed TSS approach, minimum speed steps of 10 km/h, 14 km/h and 18 km/h are found for damping ratios $\zeta = 0.5\%$, $\zeta = 1.0\%$, and $\zeta = 2.0\%$, respectively. It is thus concluded that the minimum speed-step size that is required to obtain accurate design envelopes by the proposed TSS approach increases with damping ratio, while errors derived from poor sampling in FS approaches are less sensitive to damping.

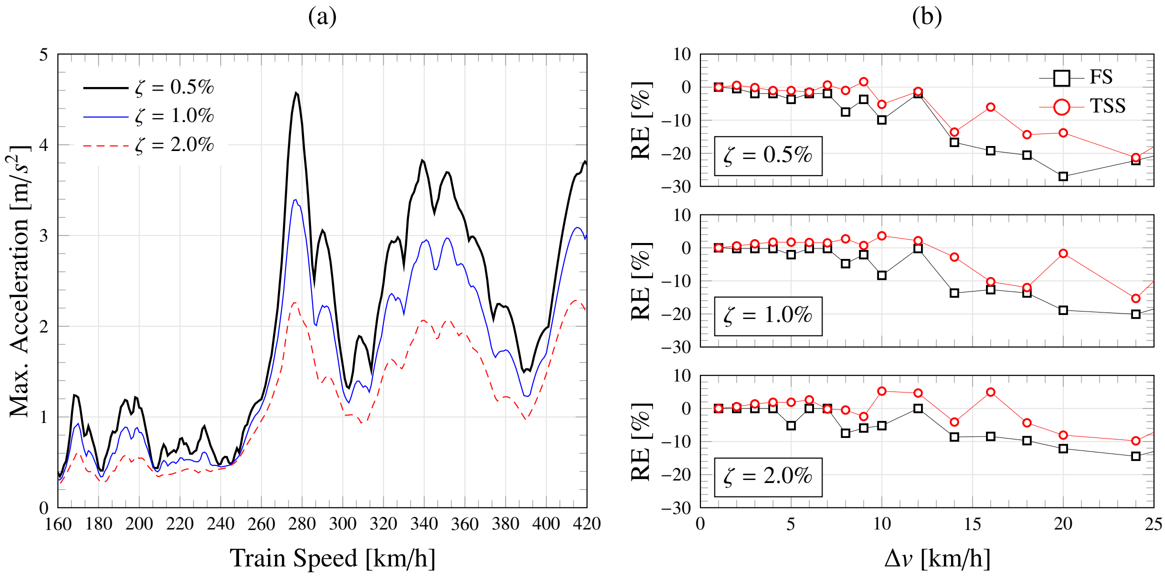

Figure 13: Maximum absolute acceleration envelopes at mid-span of the central span of the continuous three-span bridge from Eurocode 1 under the passage of the ten trains of the HSML-A model of Eurocode 1 considering different damping ratios (a), and relative error (RE) between maximum accelerations determined by the FS and TSS approaches.

4.3. Case study II: composite steel-concrete bridge, the Sesia viaduct

In this case study, the proposed meta-model is used for the dynamic analysis of a low-damped three-dimensional composite steel-concrete high-speed railway bridge, the Sesia viaduct. The Sesia viaduct is located on the Turin-Milan Italian high-speed railway line over the Novara river, and has been the subject of study of a number of research studies in the realm of Structural Health Monitoring (see e.g. [41–44]).

The bridge structure consists of seven double-track simply supported 46 m long spans, reaching a total length of 322 m. The cross-section of the bridge consists of a S355 steel double box defined by lower flanges and three webs (Fig. 14 (a)), defining a trapezoidal profile of widths ranging from 6.95 m to 9 m and depth of 3.35 m. The steel box is formed by three different segments per span, each about 15 m long and joined together by full penetration butt welds. In addition, the steel girder is reinforced by 13 intermediate and 2 end cross diaphragms per span at a spacing of 3.11 m, which provide lateral stiffness to limit the distortion of the cross-sections. The steel girder supports a concrete slab with geometrical dimensions of 13.6 m width and 0.4 m thickness through stud connections in the top flanges of the girder. Finally, the superstructure of the track consists of UIC-60 rails supported by prestressed concrete sleepers periodically spaced every 0.6 m. The bearings scheme is sketched in Fig. 14 (b) and consists of two fix bearings, one mono-directional and three bi-directional supports. A thorough description of the bridge structure can be found in reference [43].

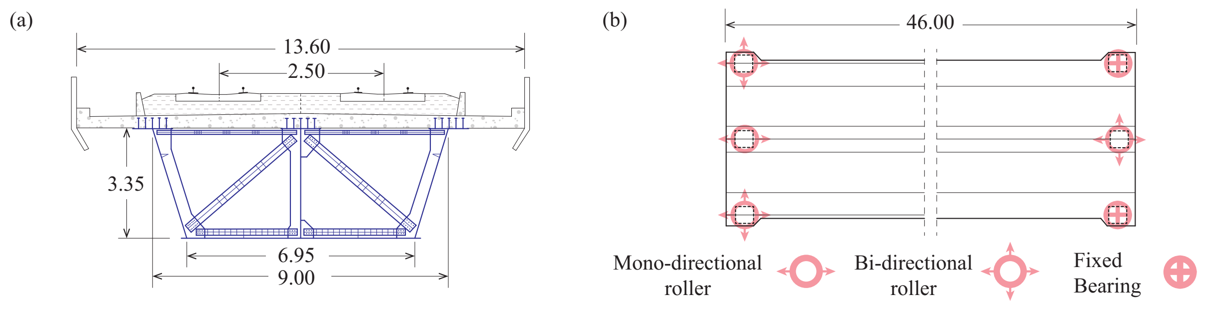

Figure 14: Cross-section of the box girder (a) and bearings layout (b) of the Sesia viaduct (units in m).

The dynamic analysis of the bridge under moving train loads requires an elevated number of simulations to accurately trace the maximum response envelopes. Given the high complexity of the bridge structure, such analyses entail considerable computational costs and memory requirements. This case study is, thus, a particularly well-suited example to illustrate the usefulness of techniques for fast evaluation of maximum response envelopes such as the meta-model proposed in this work.

4.3.1. *Finite element modelling*

In a similar way to the previous case studies, a FE model of the bridge structure is developed in the commercial code SAP2000 in order to extract the modal features. Due to the large size of the viaduct, the modelling of the seven simply-supported spans requires exorbitant computational demands. For this reason, a simplified FE model of one single span is used in this work with the boundary conditions shown in Fig. 14 (b). In order to simulate the continuity of the track superstructure, as well as to avoid the appearance of fictitious impacts at the entrance of trains, the longitudinal displacements and rotations are also constrained at the extremes of the rails. The steel box girder is divided into two 15 m long lateral segments and a 15.2 m long central one. In the lateral segments, the webs and bottom flanges are modelled by shell elements with thicknesses of 20 mm and 25 mm, respectively. The webs and bottom flanges of the central segment are also modelled by shell elements with thicknesses of 18 mm and 30 mm, respectively. The top flanges of the steel girder are modelled with 25 mm thick shell elements along the whole span. Furthermore, beam elements are used for the modelling of the diagonal and horizontal braces, as well as the longitudinal stiffeners. The concrete deck is modelled with 0.4 m thick orthotropic shell elements, considering an increase of 20% in the bending stiffness in the transverse direction. In this way, it is intended to account for the effect of the higher steel reinforcement density in the transverse direction of the deck. The connection of the concrete deck with the steel girder is simulated with massless infinitely rigid studs. The resulting FE model of the bridge is shown in Fig. 15 and contains 3280 beam elements, 12304 shell elements and 13152 nodes. Finally, the material properties used in the FE model are summarized in Table 1. Note that the mass density of steel is increased up to 8000 kg/m^3 in order to take into account the masses of welds, bolts, and all the ancillary elements that have not been explicitly defined in the model.

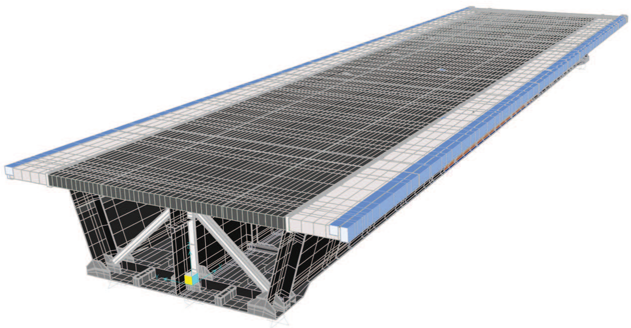

Figure 15: Perspective view of the finite element model of the Sesia viaduct.

Table 1: Material properties used in the FE modelling of the Sesia viaduct.

Item	Unit	Value
Per-unit-length mass of rails	kg/m	60.00
Mass of sleepers	kg	290.00
Young's modulus of concrete slab	MPa	31000.00
Poisson's ratio of concrete slab	-	0.17
Density of concrete slab	kg/m^3	2500.00
Young's modulus of steel girder	GPa	205.00
Poisson's ratio of steel girder	-	0.3
Density of steel girder	kg/m^3	8000.00

The modal properties of the bridge structure are extracted from a modal analysis of the developed FE model. In order to validate the numerical model, Table 2 furnishes the comparison of the first three computed modal frequencies against previously reported results in the literature. In particular, the experimental results reported by Zhou *et al.* [42], along with the numerical results reported by Guo *et al.* [41] and Liu *et al.* [45] are used for comparison. The first three natural modes are shown in Fig. 16 and correspond to a first bending mode, a first torsional mode and a second bending mode, respectively. It is observed in Table 2 that the differences of the present numerical frequencies with the experimental ones reported by Zhou *et al.* [42] are below 10% and, therefore, the developed FE model is considered suitable for the purpose of the present work. Subsequently, the natural modes with resonant frequencies below 30 Hz are retained for the dynamic analysis which, in this case, amount to the first 82 modes.

Table 2: Comparison of numerical natural frequencies of the viaduct of Sesia against previously reported results in the literature.

Vibration mode	Natural frequencies [Hz]			
	Ref. [42]	Ref. [41]	Ref. [45]	Present study
First bending mode	4.14	4.20	4.15	4.19
First torsional mode	9.00	9.30	9.01	9.68
Second bending mode	10.44	11.69	10.27	10.83

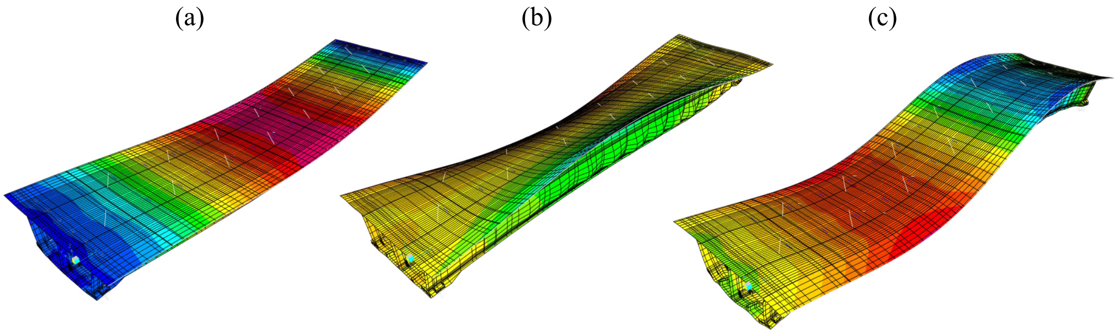

Figure 16: First bending mode (4.19 Hz) (a), first torsional mode (9.68 Hz) (b), and second bending mode (10.83 Hz) (c) of the Sesia viaduct.

4.3.2. Dynamic analysis results

On the basis of the previously computed modal features, this section reports the application of the proposed TSS meta-model to analyse the dynamic response of the Sesia viaduct under train moving loads. Firstly, the maximum absolute accelerations of the centre of the deck at mid-span are computed under the passage of the A1 train of the HSML-A model. The train loads are applied in the centreline of one of the railway tracks 2.5 m far from the centre of the deck. As commonly assumed in the design of steel-concrete composite bridges, a constant modal damping ratio of ζ=0.5% is selected in this case study. Firstly, Fig. 17 (a) depicts the maximum absolute accelerations considering two train speed increments for the TSS meta-model, namely Δv=10 km/h and 20 km/h, and a time sampling frequency of Δt=T_{min}/10=3.34 ms, with T_{min} being the minimum period of the considered vibration modes. A clear resonant train speed can be noted around v=273 km/h with a peak acceleration of 0.75 m/s^2. With regard to the results of the TSS meta-model, it is noted that the estimates are less accurate for increasing train speed increments. In the case of Δv=10 km/h, the TSS meta-model can accurately capture the peak acceleration (1.5% error), while larger differences are found at non-resonant train speeds. The estimates of the TSS meta-model with Δv=20 km/h show a similar trend. Nevertheless, the computed peak acceleration is considerably lower in this case (0.57 m/s^2, 32% error) due to an insufficient sampling of the train speed range. On the other hand, Fig. 17 (b) shows the maximum absolute accelerations considering Δv=10 km/h and two time sampling frequencies, namely is Δt=T_{min}/10 and T_{min}/100. It is clearly observed that the determination of the train speed sensitivity is notably enhanced in the case of Δt=T_{min}/100 at non-resonant speeds, while only limited enhancements are found at the resonant train speed. In line with the discussion of the previous case studies, these results illustrate the structure of the analytical solution of the sensitivity of bridge accelerations to the train speed. On the basis of the modal decomposition of the dynamic response, the sensitivity of accelerations to the train speed depends upon the square of the modal frequencies and, therefore, so are the errors in the determination of the sensitivity at maximum accelerations. At resonant speeds, only a few modes are determinant in the response and, therefore, such sampling errors are minimized.

The effectiveness of the proposed TSS meta-model can be assessed in terms of computation time. With regard to the analyses reported in Fig. 17, the computational times of the considered cases yield:

- Semi-analytic solution (Δv = 1 km/h, Δt = $T_{min}/10$) = 1388.29 s
- TSS (Δv = 10 km/h, Δt = $T_{min}/10$) = 163.63 s (reduction of 88%)
- TSS (Δv = 20 km/h, Δt = $T_{min}/10$) = 89.67 s (reduction of 94%)

which, in light of the accuracy levels reported in Fig. 17, highlight the usefulness of the proposed meta-model to obtain fast evaluations of the maximum responses of high-speed railway bridges.

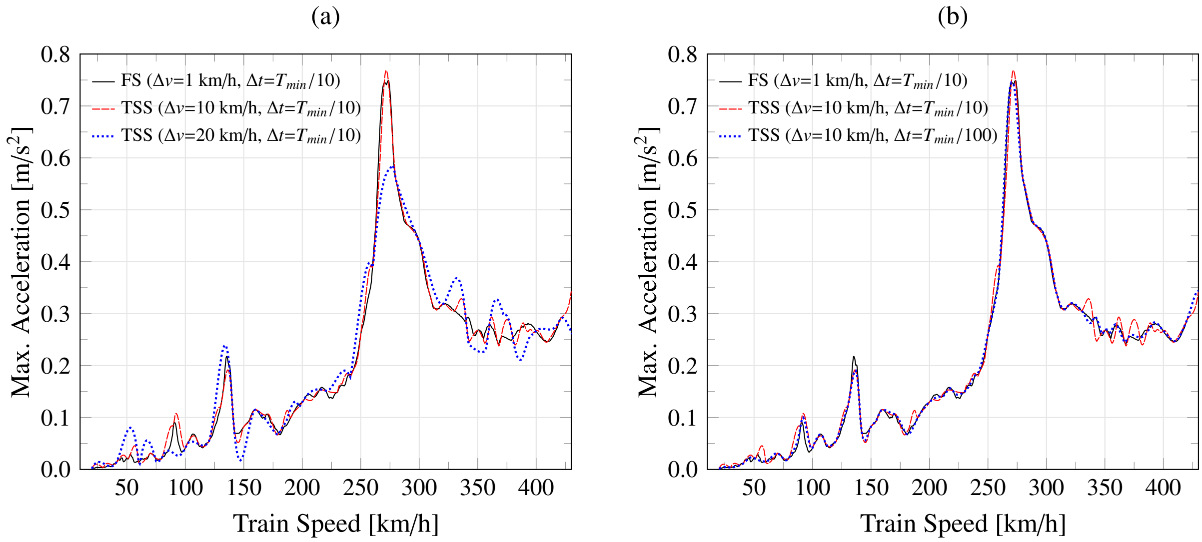

Figure 17: Maximum absolute envelopes of accelerations of the Sesia viaduct as functions of the train speed under the passage of the A1 train of the HSML-A model of Eurocode 1, considering different train speed increments (a) and time sampling frequencies (b). The accelerations are computed in the centreline of the ballast at mid-span (ζ=0.5%).

Finally, in order to further the analysis on the influence of damping on the dynamic response and the accuracy of the TSS meta-model, Fig. 18 investigates the response of the bridge in terms of maximum accelerations considering the classical Rayleigh damping. To this aim, the damping ratios reported in the experimental study of Liu *et al.* [45] are used for the first two natural frequencies. Particularly, damping ratios of ζ_1=2.17% and ζ_2=1.84% are selected for the first two modes of vibration (see Fig. 16). It is observed that the differences of the estimates of the TSS meta-model and the actual envelope are minimal in this case, yielding errors in the determination of the peak acceleration of 0.88% and 3.50% for Δv=10 km/h and 20 km/h, respectively. Due to the consideration of the classical Rayleigh damping, only a few modes of vibration remain low-damped while higher damping ratios are assumed for the rest of the modes. Hence, at resonant train speeds, lesser modes of vibration are determinant in comparison to those in the case of constant modal damping and, as a result, the errors stemming from insufficient sampling of the train sensitivity are minimized.

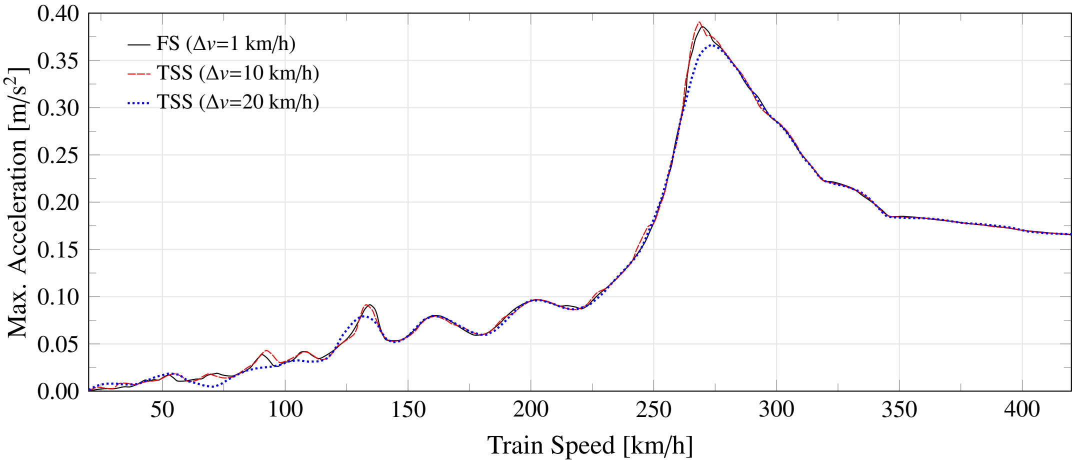

Figure 18: Maximum absolute envelopes of accelerations of the Sesia viaduct as functions of the train speed under the passage of the A1 train of the HSML-A model of Eurocode 1, considering different train speed increments and Rayleigh's damping. The accelerations are computed in the centreline of the ballast at mid-span ($\Delta_t = T_{min}/10$).

4.4. Case study III: concrete box girder bridge, the Rodenillo viaduct.

This last test copes with the dynamic analysis of a three-dimensional double-track U-shaped girder high-speed railway bridge, the Rodenillo viaduct. This test is aimed at demonstrating the effectiveness of the proposed TSS meta-model to provide fast evaluations of the maximum response envelopes of a complex three-dimensional bridge structure, including a strong influence of torsional modes.

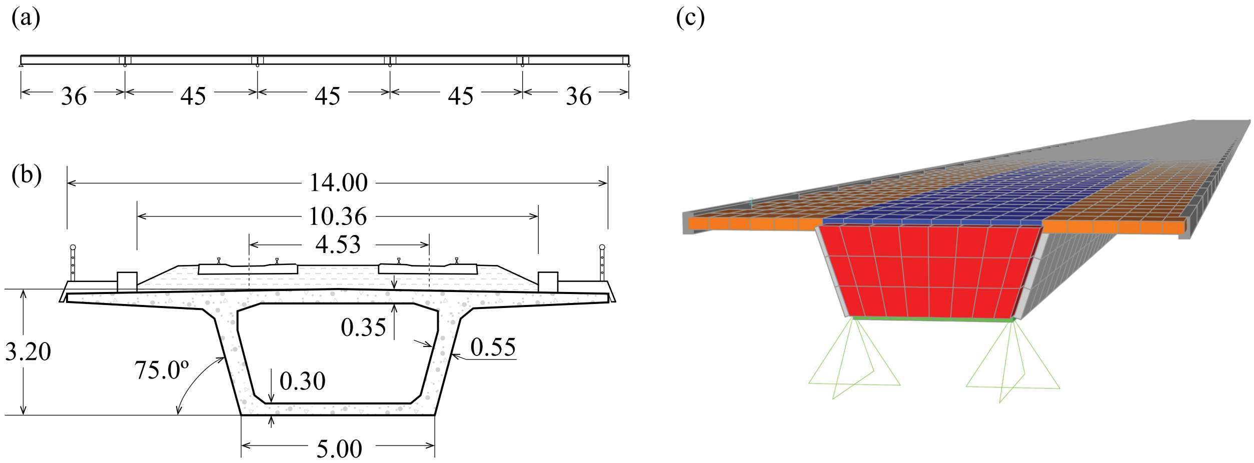

Figure 19: Lateral view (a), cross-section (b), and FE model of the viaduct of Rodenillo (c) (Units in m).

The Rodenillo viaduct is a cast-in-place concrete post-tensioned box-girder bridge located on the high-speed railway line Madrid-Valencia in Spain. The bridge consists of five continuous spans with a total length of 207 m, including two 36 m long lateral spans and three 45 m long central spans (see Fig. 19 (a)). The superstructure consists of a single-cell box cross-section with a depth of 3.1 m with 3.9 m long cantilevers on both sides, defining a 14 m long concrete deck. The thicknesses of the bottom and top flanges are 0.3 m and 0.35 m, respectively, and the webs are 0.5 m thick (see Fig. 19 (b)). In addition, the girder is reinforced by two 0.5 m thick concrete diaphragms at the supports. Finally, the superstructure of the track consists of UIC-60 rails, prestressed concrete sleepers spaced every 0.6 m, and a 0.50 m thick ballast layer.

4.4.1. Finite element model

In order to extract the modal features of the structure, the viaduct is modelled in in the commercial FE code SAP2000 (see Fig. 19 (c)). To do so, shell elements are used to model the concrete girder, including six different sections, namely 0.5 m thick webs, 0.3 m thick top flanges, 0.35 m thick bottom flanges, 0.5 m thick diaphragms and 0.35 m thick concrete cantilevers. In order to account for the effect of the higher steel reinforcement density in the transverse direction of the viaduct deck, the bending stiffness of the deck shells is increased by 20% as a common approximation in practice. Furthermore, the ballast barriers are modelled with frame elements with rectangular cross-section of 0.2×0.5 m^2. The material properties used in the model are collected in Table 3. Overall, the FE model has 38 frames and 7422 shells. The spans are defined as simply supported and, therefore, the boundary conditions consider translational fixed bearings at the first abutment, while vertical displacements are constrained in the rest of supports. Additionally, the longitudinal displacements and rotations are also constrained at the extremes of the rails to simulate the connection with the adjacent lanes. In this way, smooth load lanes are achieved and the appearance of fictitious impacts at the entrance of trains into the structure is avoided.

Table 3: Material properties used in the FE modelling of the viaduct of Rodenillo.

Item	Unit	Value
Per-unit-length mass of rails	kg/m	60.0
Mass of sleepers	kg	290.0
Mass density of ballast	kg/m^3	1800.0
Young's modulus of concrete	GPa	35.0
Poisson's ratio of concrete	-	0.2
Mass density of concrete	kg/m^3	2403.0

Finally, the FE model is used to extract the modal features of the bridge through a modal analysis in SAP2000. Fig. 20 furnishes the first three modes of vibration, including a first and second bending modes and a first torsional mode with resonant frequencies of 2.58 Hz, 2.93 Hz and 6.24 Hz, respectively. In the following, a total of 123 modes of vibration with resonant frequencies below 30 Hz are retained in the dynamic analyses. With regard to the damping of the structure, a constant modal damping ratio of ζ=2% is selected according to the Spanish code IAPF-07 [34].

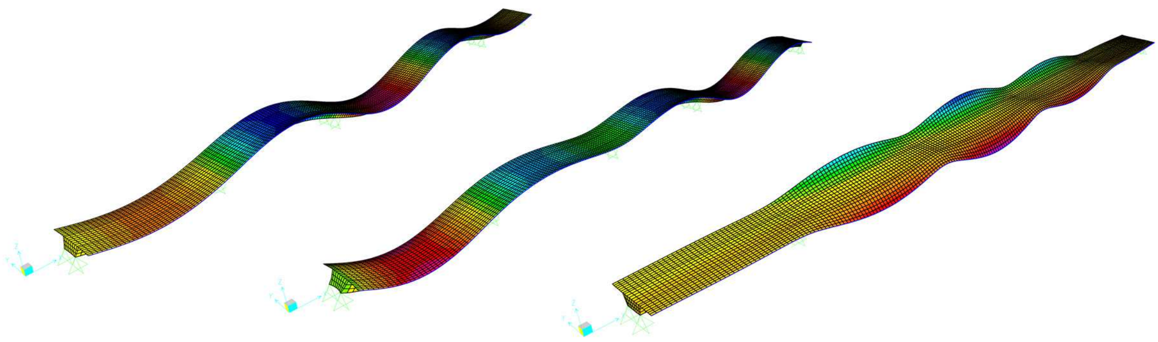

(a) (b) (c)

Figure 20: Numerical modes of vibration of the viaduct of Rodenillo: (a) first bending mode (2.58 Hz), (b) second bending mode (2.93 Hz), and (c) first torsional mode (6.24 Hz).

4.4.2. Dynamic analysis results

On the basis of the modal features extracted from the FE model, the proposed TSS meta-model is used to compute the dynamic response of the viaduct of Rodenillo. For comparison purposes, the results provided by the semi-analytic solution are also presented considering small train speed increments of 1 km/h. Figs. 21 (a) and (b) show the maximum absolute displacement and acceleration envelopes, respectively, as functions of the train speed under the passage of the A1 train of the HSML-A model of Eurocode 1. The train loads are applied in the centreline of one of the railway tracks 2.265 m far from the centre of the deck. Due to space constraints, the results in terms of maximum displacements are only shown for the critical point located at the centre of the deck at a quarter-span of the first 45 m long span. Also, the acceleration results are only shown for the point located at the edge of the ballast layer at a quarter-span of the same span. A time sampling rate of $\Delta t = T_{min}/10 = 3.9$ ms is selected, as well as a free vibration time of six times the highest period of the structure. In order to evaluate the effectiveness of the proposed TSS meta-model, two different train speed increments have been considered, namely 10 km/h and 20 km/h. It is first noted in Fig. 21 (a) that, given that the envelope of displacements is considerably smoother, the present TSS meta-model yields very close estimates to the actual envelope. In particular, the estimates computed with a train speed increment of 10 km/h accurately capture all the local and global maxima. Conversely, the global maximum ($\approx$320 km/h) goes unnoticed for the envelope computed with a train speed increment of 20 km/h due to insufficient sampling. On the other hand, although larger differences in maximum accelerations can be observed throughout the range of considered speeds in Fig. 21 (b), these get considerably reduced at local/global maxima points. Let us recall that the train speed sensitivity in terms of accelerations is directly proportional to the square of the modal frequencies and, therefore, so are the sampling errors in the determination of the sensitivity at maximum acceleration points. Hence, at resonant trains speeds, only a few modes are determinant in the response and the sampling errors in the determination of the maximum train speed sensitivity get substantially reduced, what explains the higher accuracy of the TSS meta-model at local/global maxima points.

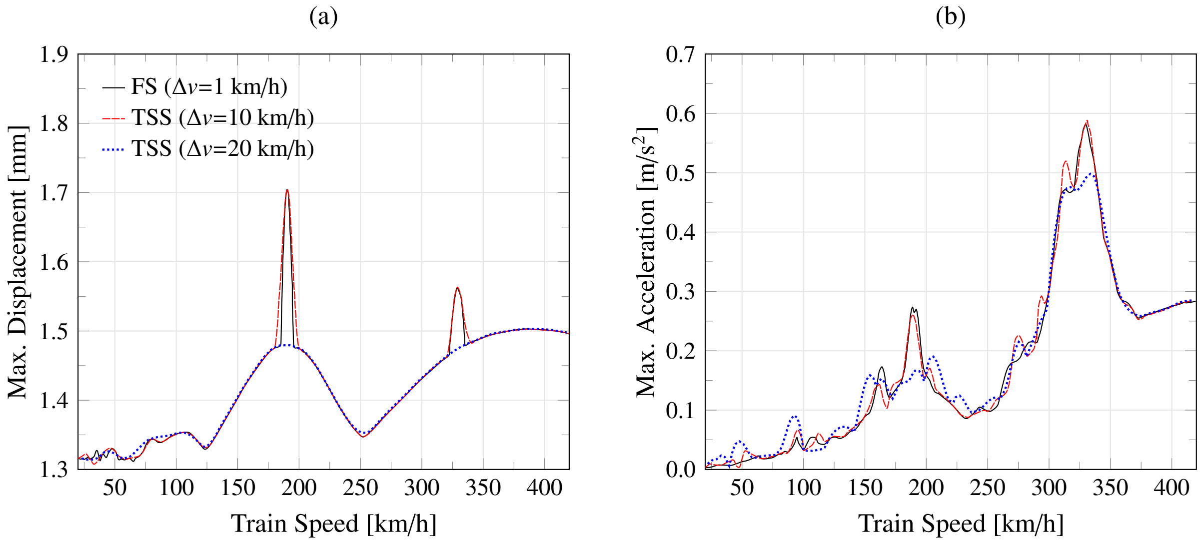

Figure 21: Maximum absolute envelopes of displacements (a) and accelerations (b) of the viaduct of Rodenillo as functions of the train speed considering different train-speed steps. Displacements and accelerations are computed in the centre of the deck and the edge of the ballast layer at the quarter-span of the first span, respectively. (Train A1 of the HSML-A model of Eurocode 1, Δt=$T_{min}/10$).

Figure 22 deepens the previous analyses on the effects of the time sampling rate on the estimates of the TSS meta-model. To do so, two different time steps are considered, namely $\Delta t = T_{min}/10 = 3.9$ ms and $T_{min}/100 = 0.39$ ms, assuming a constant train speed increment of Δv=10 km/h. Firstly, it is noted in Fig. 22 (a) that the time sampling rate has little effect on the determination of the maximum displacements. Conversely, it is observed in Fig. 22 (b) that considerably closer fittings with the semi-analytic solution are obtained for decreasing sampling frequencies. Interestingly, these differences are shown notably reduced at resonant train speeds (see e.g. 190 km/h or 320 km/h). The presented results illustrate the structure of the proposed approach and, as a result, it is concluded that the TSS meta-model provides fast evaluations of maximum response envelopes of bridge structures through the sub-sampling of the train speed range, yielding minimal differences at resonant speeds related to local/global maxima.

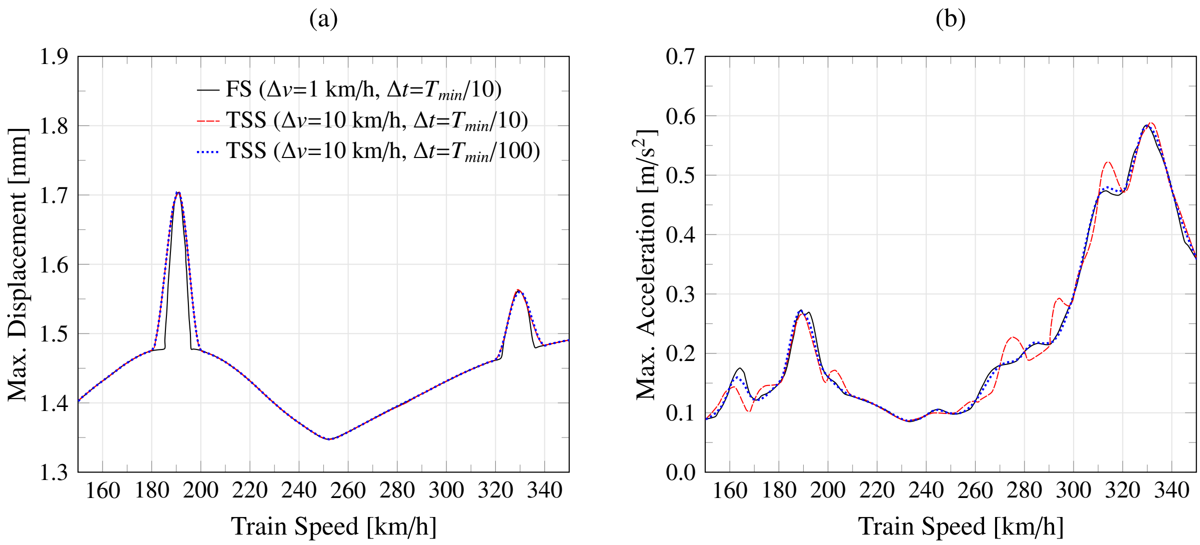

Figure 22: Maximum absolute envelopes of displacements (a) and accelerations (b) of the viaduct of Rodenillo as functions of the train speed considering different time steps. Displacements and accelerations are computed in the centre of the deck and the edge of the ballast layer at the quarter-span of the first span, respectively. (Train A1 of the HSML-A model of Eurocode 1).

Finally, Figs. and 24 show the global maximum absolute displacements and accelerations envelopes of the viaduct of Rodenillo, respectively. In this case, the ten trains of the HSML-A model, the AVE and TALGO trains are considered. The accelerations are computed at the edge of the ballast layer at the quarter-span of the first 45 m long span. The estimates provided by the TSS meta-model are computed assuming train speed increments of Δv=10 km/h and 20 km/h, and a time sampling frequency of Δt=$T_{min}/10$. It is noted that similar conclusions to the previous analyses can be also extracted in the case of maximum response envelopes considering multiple multi-point train loads. The maximum absolute accelerations provided by the semi-analytic solution and the TSS meta-model for Δv=10 km/h and 20 km/h are 0.825 m/s^2, 0.828 m/s^2 (0.35% error) and 0.890 m/s^2 (7.90% error), respectively. Hence, it is concluded the proposed TSS meta-model can efficiently provide fast evaluations of the maximum response envelopes of three-dimensional low-damped bridges under the passage of complex moving multi-point train loads, of high interest for preliminary design stages.

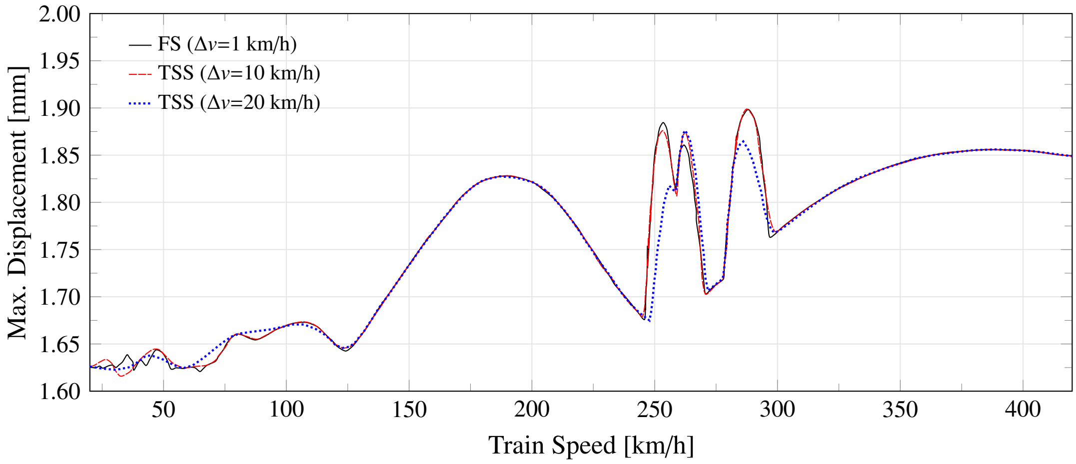

Figure 23: Maximum absolute envelopes of displacements of the viaduct of Rodenillo as functions of the train speed under the passage of the ten trains of the HSML-A model, the AVE and TALGO trains. The displacements are computed in the centre of the deck at the quarter-span of the first 45 m long span (ζ=2%, Δt=$T_{min}/10$).

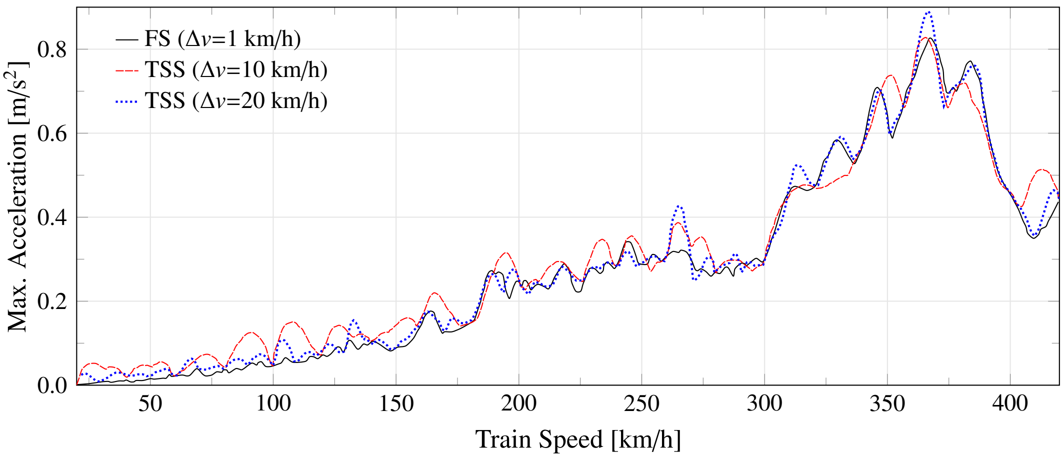

Figure 24: Maximum absolute envelope of accelerations of the viaduct of Rodenillo as a function of the train speed under the passage of the ten trains of the HSML-A model, along with the AVE and TALGO trains. The accelerations are computed at the edge of the ballast layer at the quarter-span of the first 45 m long span (ζ=2%, Δt=$T_{min}/10$).

Finally, in a similar way to the previous case study, the effectiveness of the proposed TSS meta-model can be assessed in terms of computation time. In this case, the computational times required to obtain the results previously shown in Figs. 23 and 24 are the following ones:

- Semi-analytic solution (Δv = 1 km/h, Δt = $T_{min}/10$) = 10518.56 s
- TSS (Δv = 10 km/h, Δt = $T_{min}/10$) = 1120.78 s (reduction of 89%)
- TSS (Δv = 20 km/h, Δt = $T_{min}/10$) = 608.53 s (reduction of 94%)

These results demonstrate the usefulness of the proposed meta-model which, while providing reasonably good estimates of the maximum dynamic responses of the bridge, yield considerable reductions in the computation times. Such reductions can be particularly beneficial during pre-design stages, where the TSS meta-model can provide fast evaluations of the dynamic response of diverse design alternatives.

5. Conclusions

In this paper, a novel approach for fast assessment of maximum response envelopes of railway bridges under moving train loads has been presented. The proposed TSS meta-model is based on the train speed sensitivity of the dynamic response envelope curves. Specifically, this technique tracks the maximum values of the dynamic response of the structure (displacements or accelerations) along with their sensitivity to train speed variations. On the basis of the semi-analytic solution of the time-dependent modal equations, the present approach also computes the train speed sensitivity in closed-form. Considering the computed slopes, it is possible to define a moderate sampling frequency of the design range of train speeds and, afterwards, approximate the non-sampled speeds through a cubic spline interpolation. The proposed technique, implemented in a FORTRAN computer code, has proven computationally efficient on a standard desktop PC. Four numerical case studies have been presented to illustrate the potentials of the proposed methodology. Overall, the numerical results have demonstrated substantial reductions in the computation times. Additionally, the proposed cubic interpolation has been shown capable of sufficiently approximating the maximum response envelopes. In particular, accurate approximations have been reported at resonant train speeds where only a limited number of modes are activated. This feature allows structural engineers to rapidly assess and compare the performance of different structural alternatives at early design stages. On the whole, the key features of the present methodology can be listed as follows:

- On the basis of the semi-analytic solution of the dynamic equations of motion, the time-dependent train speed sensitivity of the solution has been also derived in closed-form. Alike the semi-analytic solution, the proposed methodology is highly accurate and robust because no time integration errors are involved.
- The only approximation introduced in the procedure stems from the spatial discretization of the structure through the FE modelling.
- In virtue of the envelope theorem, the slopes of the design envelopes are evaluated at instant times where local maxima are found. Hence, at every train speed, the TSS must be only computed and stored at instant times of local maxima.
- A time step is required in order to plot the time-history of the response. Although the solution is analytical in the time domain, sampling errors may arise in the determination of local maxima and, as a result, in the slope of the maximum response envelopes. Nevertheless, the numerical results have demonstrated that sampling errors are minimized at resonant speeds where only a few modes are activated.

Future developments of the proposed meta-model include the evaluation of different regression models to interpolate the non-sampled train speeds. Leveraging the closed-form analytical definition of the problem in the time domain, higher order sensitivities can be also obtained in closed form and, as a result, new enriched interpolation approaches may be explored for the fast assessment of maximum response design envelopes for high-speed railway bridges.

Acknowledgement

The authors wish to express their gratitude to Dr. Pedro Museros (Department of Continuum Mechanics and Theory of Structures, Polytechnical University of Valencia) for his contributions in the original development, ideas, and code used to solve the forward problem by the semi-analytic solution, and also to Mr. Alejandro Castillo-Linares (CEO of ACL-Estructuras) providing real data in the Rodenillo viaduct.

This work is part of the project TEP-5066, “Monitorización Estructural predictiva en puentes ferroviarios de alta velocidad”, Junta de Andalucía (Spain). The financial support is gratefully acknowledged.

References

[1] European Commission. Directorate General for Mobility, High-speed Europe: A Sustainable Link Between Citizens, Publications Office of European Union, 2010.

[2] L. Mao, Y. Lu, Critical speed and resonance criteria of railway bridge response to moving trains, Journal of Bridge Engineering 18 (2011) 131–141.

[3] S. Schneider, S. Marx, Design of railway bridges for dynamic loads due to high-speed traffic, Engineering Structures 174 (2018) 396–406.

[4] European Rail Research Institute (ERRI), Project D–214: Rail bridges for speeds > 200 km/h. Final Report (RP9), Technical Report, 2001.

[5] M. Majka, M. Hartnett, Dynamic response of bridges to moving trains: A study on effects of random track irregularities and bridge skewness, Computers & Structures 87 (2009) 1233–1252.

[6] European Committee for Standardization (CEN), Eurocode 1: Actions on structures - part 2: Traffic loads on bridges, EN 1991-2 Eurocode 1 (2003).

[7] European Committee for Standarization (CEN), EN 1990 - Eurocode: Basis of structural design - Annex A2: Application for bridges, Final PT Draft EN 1990 - prAnnex A2, 2002.

[8] L. Deng, Y. Yu, Q. Zou, C. S. Cai, State-of-the-art review of dynamic impact factors of highway bridges, Journal of Bridge Engineering 20 (2014) 04014080.

[9] L. Frỳba, A rough assessment of railway bridges for high speed trains, Engineering structures 23 (2001) 548–556.

[10] E. Savin, Dynamic amplification factor and response spectrum for the evaluation of vibrations of beams under successive moving loads, Journal of Sound and Vibration 248 (2001) 267–288.

[11] S. A. Hamidi, F. Danshjoo, Determination of impact factor for steel railway bridges considering simultaneous effects of vehicle speed and axle distance to span length ratio, Engineering Structures 32 (2010) 1369–1376.

[12] Manual, AREMA, American railway engineering and maintenance-of-way association (2006).

[13] J. M. Goicolea, J. Dominguez, J. A. Navarro, F. Gabaldon, New dynamic analysis methods for railway bridges in codes IAPF and Eurocode 1, Railway Bridges Design, Construction and Maintenance, Madrid (2002) 1–43.

[14] M. Zacher, M. Baeßler, Dynamic behaviour of ballast on railway bridges, in: Dynamics of High–Speed Railway Bridges. Selected and revised papers from the Advanced Course on 'Dynamics of High–Speed Railway Bridges', Porto, Portugal, 20–23 September 2005, CRC Press, 2008.

[15] Commitee ERRI D-214. Design of Railway Bridges for Speed up to 350 km/h; Dynamic loading effects including resonance: Final report. Draft C., 1998.

[16] Commitee ERRI D-214.2. Utilisation de convois universels pour le dimensionement dynamique de ponts-rails. Synthèse des résultats du D214.2: Rapport final., 2002.

[17] P. Norris, T. Wilkins, I. Bucknall, Permissible deck accelerations for rail bridge dynamic assessments, volume 87, International Association for Bridge and Structural Engineering, 2003, pp. 52–58.

[18] H. Xia, N. Zhang, Dynamic analysis of railway bridge under high-speed trains., Computer and Structures. 81 (2003) 2467–2478.

[19] C. Rebelo, L. S. da Silva, C. Rigueiro, M. Pircher, Dynamic behaviour of twin single-span ballasted railway viaducts–field measurements and modal identification, Engineering Structures 30 (2008) 2460–2469.

[20] F. Bleich, Theorie und Berechnung der Eisernen Brücken, Springer, 1924.

[21] L. Frỳba, Dynamics of railway bridges, Thomas Telford, 1996.

[22] L. Frỳba, Vibration of solids and structures under moving loads. 3rd ed., Thomas Telford, 1999.

[23] J. S. Wu, L. K. Chiang, Dynamic analysis of an arch due to a moving load, Journal of Sound and Vibration 269 (2004) 511–534.

[24] S. H. Li, J. Y. Ren, Analytical study on dynamic responses of a curved beam subjected to three-directional moving loads, Applied Mathematical Modelling 58 (2018) 365–387.

[25] J. J. Wu, Dynamic analysis of an inclined beam due to moving loads, Journal of Sound and Vibration 288 (2005) 107–131.

[26] F. R. Rofooei, A. Enshaeian, A. Nikkhoo, Dynamic response of geometrically nonlinear, elastic rectangular plates under a moving mass loading by inclusion of all inertial components, Journal of Sound and Vibration 394 (2017) 497–514.

[27] B. Dyniewicz, D. Pisarski, C. I. Bajer, Vibrations of a Mindlin plate subjected to a pair of inertial loads moving in opposite directions, Journal of Sound and Vibration 386 (2017) 265–282.

[28] P. Malekzadeh, A. R. Fiouz, H. Razi, Three-dimensional dynamic analysis of laminated composite plates subjected to moving load, Composite Structures 90 (2009) 105–114.

[29] Q. Song, Z. Liu, J. Shi, Y. Wan, Parametric study of dynamic response of sandwich plate under moving loads, Thin-Walled Structures 123 (2018) 82–99.

[30] C. G. Koh, G. H. Chiew, C. C. Lim, A numerical method for moving load on continuum, Journal of Sound and Vibration 300 (2007) 126–138.

[31] Z. Y. Ai, C. J. Xu, G. P. Ren, Vibration of a pre-stressed plate on a transversely isotropic multilayered half-plane due to a moving load, Applied Mathematical Modelling 59 (2018) 728–738.

[32] H. Ouyang, Moving-load dynamic problems: A tutorial (with a brief overview), Mechanical Systems and Signal Processing 25 (2011) 2039 – 2060.

[33] A. Martínez-Castro, P. Museros, A.Castillo-Linares, Semi-analytic solution in the time domain for non-uniform multi-span Bernoulli-Euler beams traversed by moving loads, Journal of Sound and Vibration 294 (2006) 278–297.

[34] Instrucción de acciones a considerar en en el proyecto de puentes de ferrocarril (IAPF), 2007.

[35] P. Museros, A. Martínez-Castro, A.Castillo-Linares, Semi-analytic solution for Kirchhoff plates traversed by moving loads, in: Proceedings of the 6th International Conference on Structural Dynamics. EURODIN 2005, Paris, France, pp. 1619–1624.

[36] A. Martínez-Castro, E. García-Macías, Two techniques for fast evaluation of design envelopes in high-speed train railway bridges: Train speed sensitivity and the Hilbert Transform., in: Proceedings of the 9th International Conference on Structural Dynamics. EURODYN 2014, Porto, Portugal, pp. 1309–1314.

[37] C. P. Simon, L. Blume, Mathematics for economists, volume 7, Norton New York, 1994.

[38] T. M. Apostol, Mathematical analysis, Addison Wesley Publishing Company, 1974.

[39] P. Milgrom, I. Segal, Envelope theorems for arbitrary choice sets, Econometrica 70 (2002) 583–601.

[40] K. Henchi, M. Fafard, G. Dhatt, M. Talbot, Dynamic behaviour of multi-span beams under moving loads, Journal of Sound and Vibration 199 (1997) 33–50.

[41] W. W. Guo, H. Xia, G. De Roeck, K. Liu, Integral model for train-track-bridge interaction on the Sesia viaduct: Dynamic simulation and critical assessment, Computers & Structures 112 (2012) 205–216.

[42] H. Zhou, K. Liu, G. Shi, Y. Q. Wang, Y. J. Shi, G. De Roeck, Fatigue assessment of a composite railway bridge for high speed trains. Part I: Modeling and fatigue critical details, Journal of Constructional Steel Research 82 (2013) 234–245.

[43] H. Zhou, G. Shi, Y. Wang, H. Chen, G. De Roeck, Fatigue evaluation of a composite railway bridge based on fracture mechanics through global-local dynamic analysis, Journal of Constructional Steel Research 122 (2016) 1–13.

[44] K. Matsuoka, A. Collina, M. Sogabe, Dynamic simulation and critical assessment of a composite bridge in high-speed railway, Procedia Engineering 199 (2017) 3027–3032.

[45] K. Liu, E. Reynders, G. D. Roeck, G. Lombaert, Experimental and numerical analysis of a composite bridge for high-speed trains, Journal of Sound and Vibration 320 (2008) 201–220.